Chapter 12 High-Pressure Phase Equilibria

For pure fluids, critical pressures 2.3 bar to 1500 bar
The pressure at the bottom of the deepest ocean (about 10km deep) is about 1150 bar.

On the other hand, for man-made processes, high-pressure techniques can require pressures like 5 x 10^4 bar (synthesis of diamonds), or even 10^6 bar, as in explosive welding and plating, sophisticated techniques used in the production of tubing for chemical reactors.

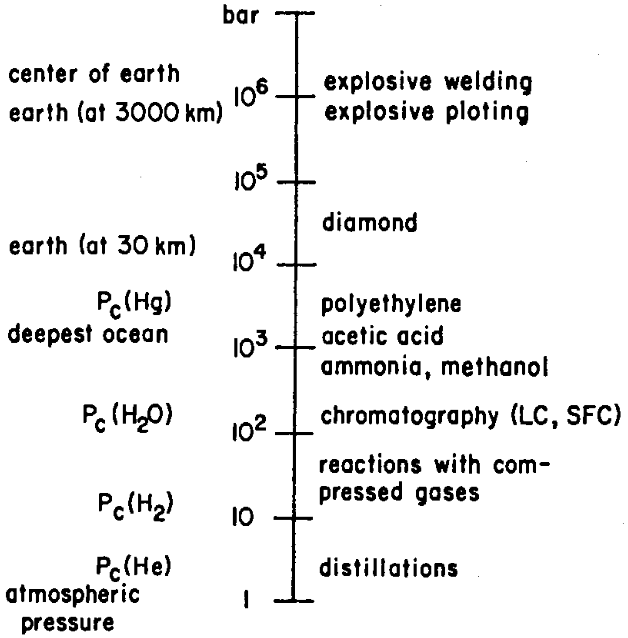

Figure 12-1 Pressure scale for natural (left) and chemical (right) processes (Schneider, 1976).

So, it is necessary to understand the thermodynamic properties of fluids at high pressures, as discussed in this chapter.

12.1 Fluid Mixtures at High Pressures

Figure 12-2 shows the relation between pressure and composition at 149℃.

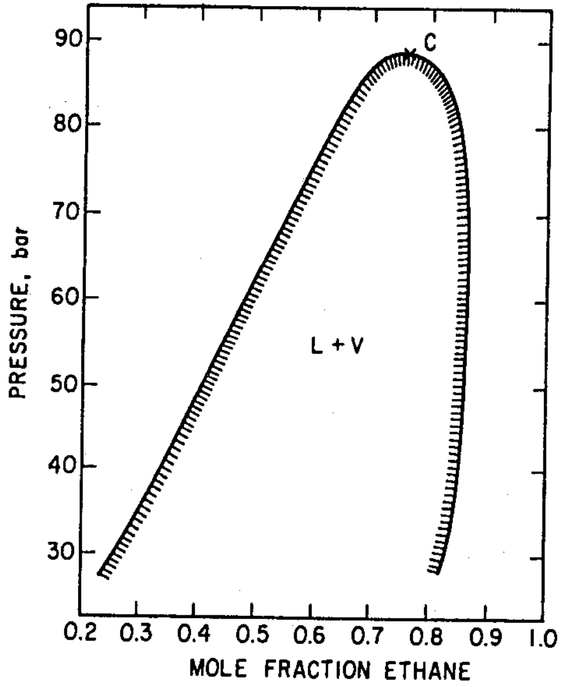

Figure 12-2 Pressure-composition diagram for the system ethane/*n*-heptane at 149°C. The critical point of the mixture is at C (Mehta and Thodos, 1965).

The left-hand line gives the saturation pressure (bubble pressure) as a function of liquid.
The right-hand line gives the saturation pressure (dew pressure) as a function of vapor.
The two lines meet at the critical point where the two phases become identical.

At 149℃ the critical composition is 76 mol % ethane and the critical pressure is 88 bar.
At this temperature and composition, therefore, only one phase can exist at pressures higher than 88 bar.

Figure 12-3 gives experimentally observed critical temperatures and pressures as a function of mole fraction for the ethane/n-heptane system. While the critical temperature of this system is a monotonic function of composition, the critical pressure goes through a maximum; many, but by no means all, binary systems behave this way

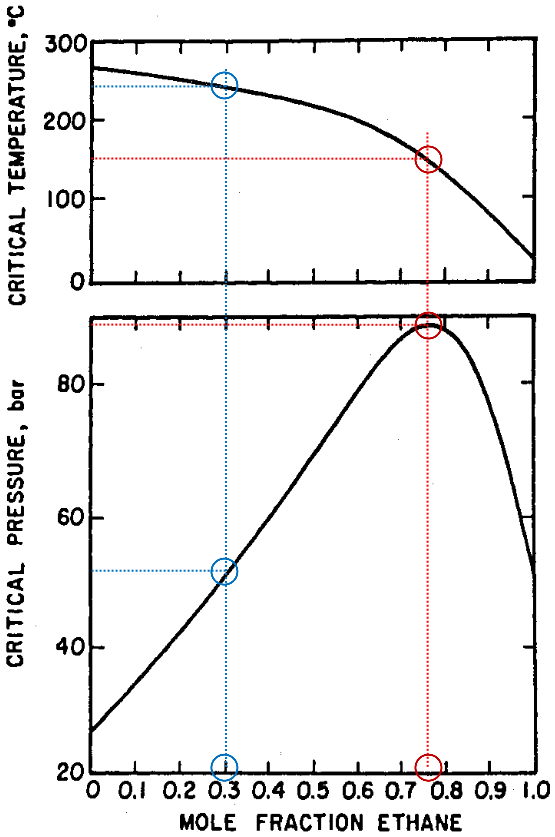

Figure 12-3 Critical temperatures and pressures for the system ethane/*n*-heptane (Mehta and Thodos, 1965).

Ex) At 76 mol % ethane, critical temperature is 149℃ and critical pressure is 88 bar.

At 30 mol % ethane, critical temperature is about 240℃ and critical pressure is about 53 bar.

For typical technical calculations it is convenient to express phase-equilibrium relations in terms of *K* factors; by definition *K*≡y/x, the ratio of the mole fraction in the vapor phase y, to that in the liquid phase x.

Figure 12-4 shows experimental K factors for the two components of the methane/propane system.

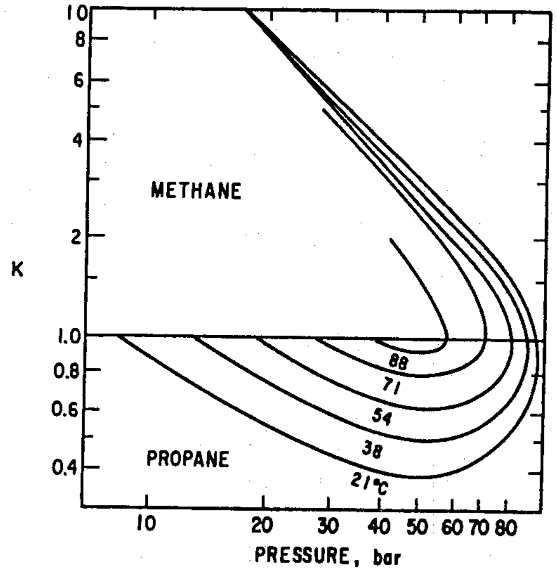

Figure 12-4 *K* factors for the methane/propane system (Sage and Lacey, 1938).

12.2 Phase Behavior at High Pressure

Basic calculation form of the phase equilibrium; for vapor-liquid equilibrium,

$$f_i^V = f_i^L$$

for every component *i* in the mixture.

Interpretation of Phase Diagrams

To interpret phase diagrams we apply the Gibbs phase rule. For nonreacting systems, that rule is expressed by the simple relation,

$$F = m + 2 - \pi \qquad (12\text{-}1)$$

where the number of independent variables (or degrees of freedom) F is related to the number of components m and number of phases π. However, at a critical point, there are additional π -1 constraints that reduce the number of degrees of freedom given by Eq. (12-1)

Three dimensional diagram in pressure, temperature and a third variable is required for a complete description of a two-component system.

Table 12-1 Geometric constraints imposed by the phase rule on phase equilibria.

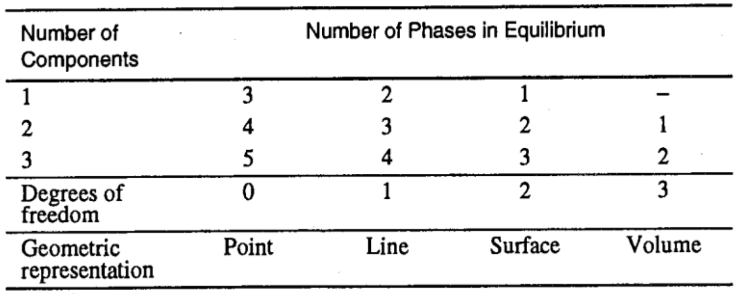

Number of Components	Number of Phases in Equilibrium			
1	3	2	1	–
2	4	3	2	1
3	5	4	3	2
Degrees of freedom	0	1	2	3
Geometric representation	Point	Line	Surface	Volume

The most convenient choice for this third variable is the composition z, where z designates the composition of a phase of any kind (solid, liquid, or gas). And three-dimensional drawings are commonly used, together with two-dimensional diagrams cut by planes of constant T or P, or formed by projections of lines and points on the P-T coordinate plane.

Classification of Phase Diagrams for Binary Mixtures

Almost binary fluid-phase equilibria can be predicted using the ‘Van der Walls EOS’ and ‘quadratic mixing rule’.

According to Van Konynenburg and Scott, binary fluid phase behaviors were classified into six types.

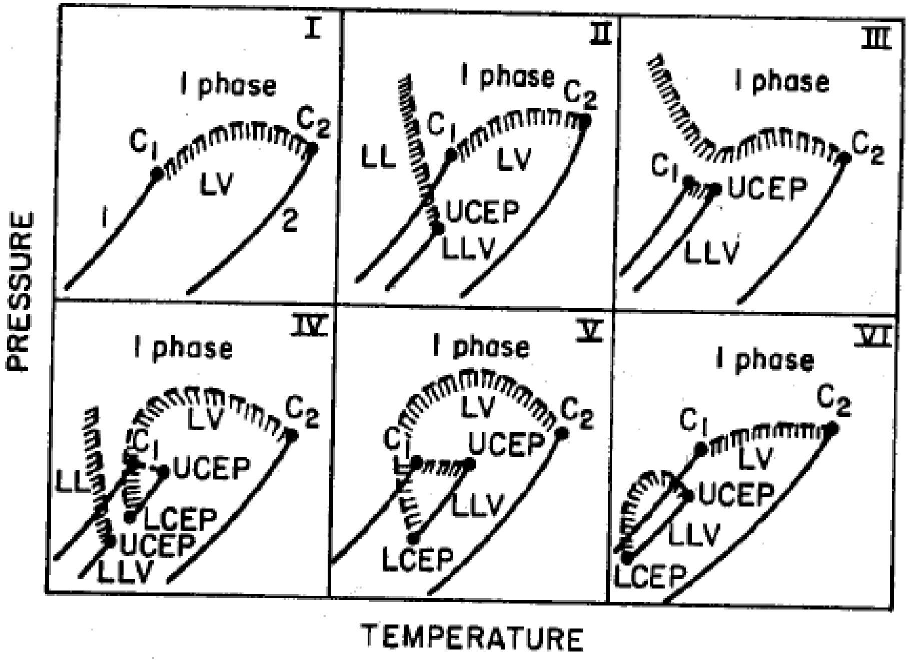

Figure 12-6 Six types of phase behavior in binary fluid systems. C = critical point; L = liquid; V = vapor; UCEP = upper critical end point; LCEP = lower critical end point. Dashed curves are critical lines and hatching marks heterogeneous regions.

Type 1-Phase Behavior

- for a typical mixture

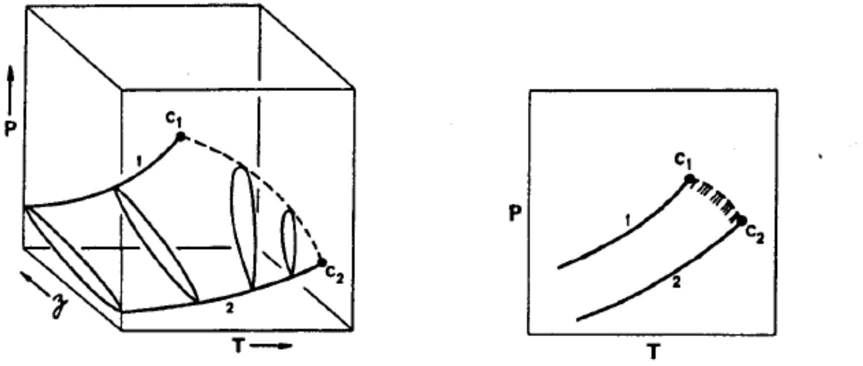

Figure 12-5 *P-T-z* surface and corresponding *P-T* projection showing vapor-liquid equilibria for a simple binary mixture (type I).

Type 2-Phase Behavior

- Similar to type 1 expet that, at low temperatures, liquid mixtures of components 1 and 2 are not miscible in all proportions.

- There is thus one additional critical line, and the line labeled LLV gives the locus of a three-phase line.

- The phase diagrams of type 2- mixtures mab be complicated by the presence of an azeotropic line.

*UCEP = uupper critical end point

Type 3-Phase Behavior

- In this type, the critical locus has two branches.

- One branch goes from the vapor-liquid critical point of the more volatile component, C1, to UCEP, where the gaseous phase and the liquid phase have the same composition.

- The other branch starts at C2 and then rises with pressure, perhaps with a positive slope or with a negative slope or with a slope that changes sign.

- The critical line starting from C2 with a positive slope indicates the existence of what is called gas-gas equilibria

- Gas-gas immiscibelity is conveniently classified as either ‘first kind’ or ‘second kind’

Type 4-Phase Behavior

- Type 4 is similar to type 5. However, in type 4 the LLV locus has two parts.

Type 5-Phase Behavior

- In type 5, the first branch of the critical line goes from C1 to UCEP as in type 3, but the second branch goes from C2 to the lower critical end point (LCEP).

- Contrarily to type 4, in type 5 mixtures, the liquids are completely miscible below LCEP.

- Figure 12-7 gives a schematic representation of what is visually observed at the LCEP and at the UCEP.

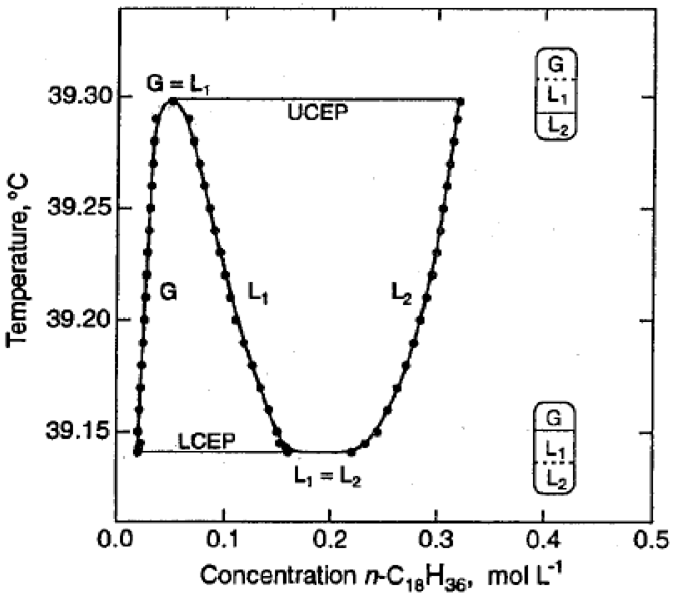

Figure 12-7 Three-phase behavior and schematic representation of critical end points for the binary ethane/*n*-octadecane (Specovius *et al.*, 1985). The dashed line represents a disappearing meniscus, i.e., a critical point: gas-liquid at the UCEP (39.30°C) and liquid-liquid at the LCEP (39.14°C).

- Type 5 behavior occurs in the system methatn/n-haxane and is also found in binaries containing alcohols. An example is provided by ethylene/methanol whose phase behavior is shown in Fig. 12-8.

- From the P-T projection represented in Figure 12-8 (a), several P-x diagrams were derived at four characteristic temperatures.

- At temperature Ti, there is a normal gas-liquid equilibrium [Figure 12-8 (b)]

- When the temperature of the LCEP is exceeded, a L1L2 region begins to grow out of the bubble curve [Figure 12-8 (c)]

- At the critical temperature of pure ethylene, froms an additional critical point [Figure 12-8 (d)]

- As the temperature increases further, L2-V region becomes smaller until it disappears at the temperature of the UCEP [Figure 12-8 (e)]

- Figure 12-9 shows experimental phase equilibrium measurements for the same binary at 260, 273, 284.15 and 2298.15 K.

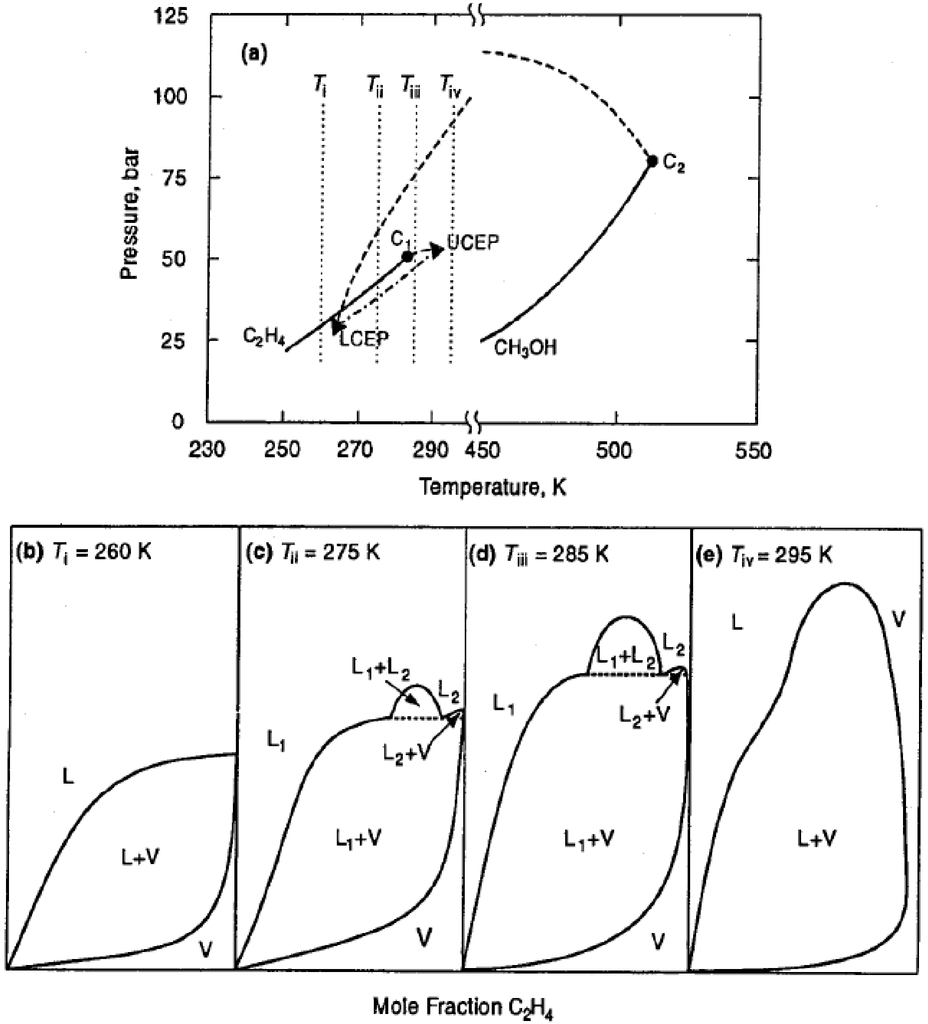

Figure 12-8 Phase-behavior of ethylene (1)/methanol (2): (a) Experimentally obtained *P-T* projection (note the scale change in the temperature axis at about 300 K, required by the large difference between the volatilities of the two components). —— Vapor-pressure curves of the pure components; - - - - critical lines; — - — - LLV three-phase line; (b) to (e) *P-x* isotherms at the temperatures indicated.

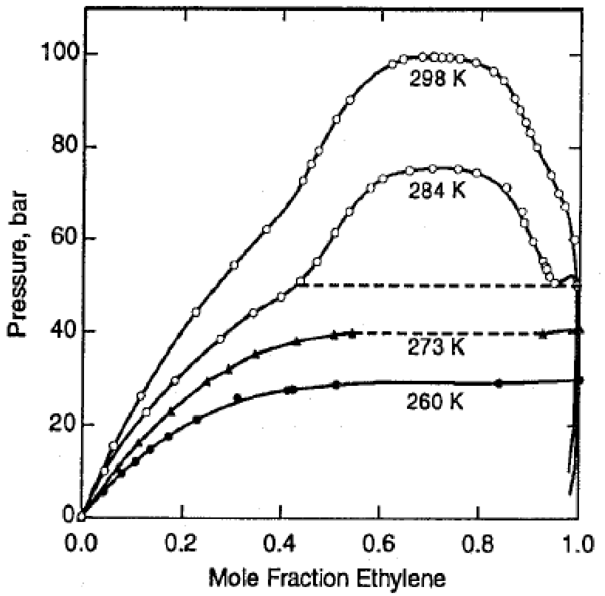

Figure 12-9 Pressure-composition phase-equilibrium data for ethylene/methanol at 260 K and 273 K (Zeck and Knapp, 1986) and at 284 K and 298 K (Brunner, 1985).

Type 6-Phase Behavior

- Finally, binary mixtures showing type 6 phase behavior have two critical curves
- One connects C1 and C2 while another connects UCEP and LCEP.
- The two critical curves meet at an upper critical pressure; at higher pressures two liquids are miscible.

Critical Phenomena in Binary Fluid Mixtures

- Figure 12-6 gives different types of pressure-temperature diagrams for binary systems for a simple binary mixtuer at fixed composition, we have a bubble-point (boiling) curve on the left and a dew-point (condensation) curve on the right, as shown in Figure 12-10.

- These two curves come together at the critical point.

- The dashed lines in Figure 12-10 are lines of constant *quality**.

* In a two-phase (vapor-liquid) mixture, quality is defined as the fracton that is in the vapor phase.

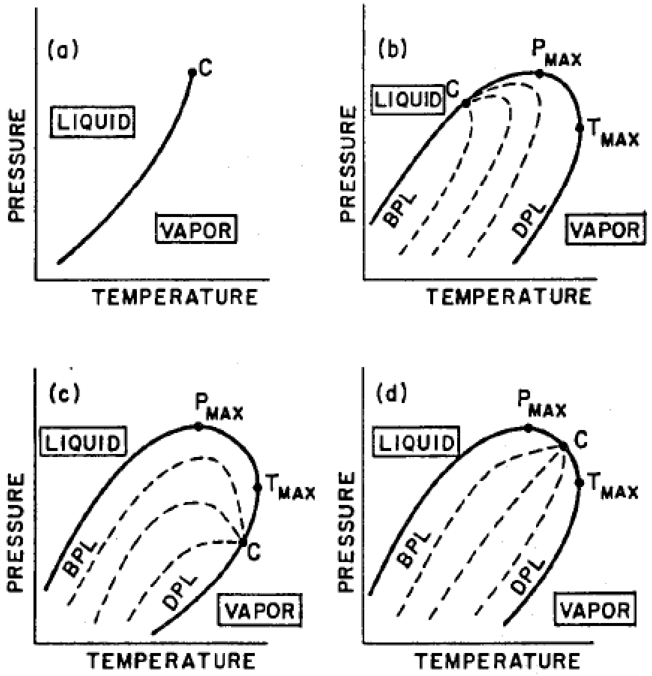

Figure 12-10 Pressure-temperature diagrams for a pure fluid (a) and for fluid mixtures at constant composition (b, c, d). BPL = bubble-point line; DPL = dew-point line; C = critical point. Dashed lines show constant quality.

- For a pure fluid, the bubble-point and dew-point curves collapse into one single line; in that event, the critical point is a maximum.

- However, in a mixture, the critical point is not necessarily a maximum with respect to either temperature or pressure.

- The relative positions of C, T_{max}, and P_{max} (see Figure 12-10) give rise to a curious but well known phenomenon : *retrograde condensation.*

In the vicinity of the mixture's critical point, isothermal compression may proceed such that an isotherm cuts the dew-point line not once, but twice and does not cut the cubble-point line at all. Such an isotherm is shown in Figure 12-11.

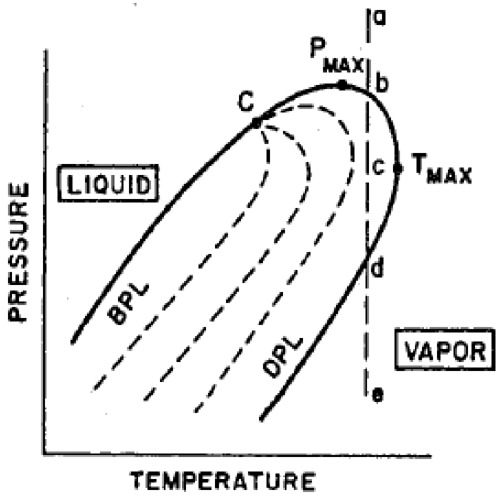

Figure 12-11 Retrograde condensation. The vertical line cuts the dew-point line twice. BPL = bubble-point line; DPL = dew-point line; C = critical point. When gaseous mixture *e* is compressed isothermally, liquid begins to form at *d*; maximum condensation occurs at *c*, and at *b*, all condensate is vaporized. Dashed lines show constant quality.

- Phase behavior of liquid mixtures containing only subcritical components is also affected by pressure, but in this case much higher pressures are usually required to produce significant changes

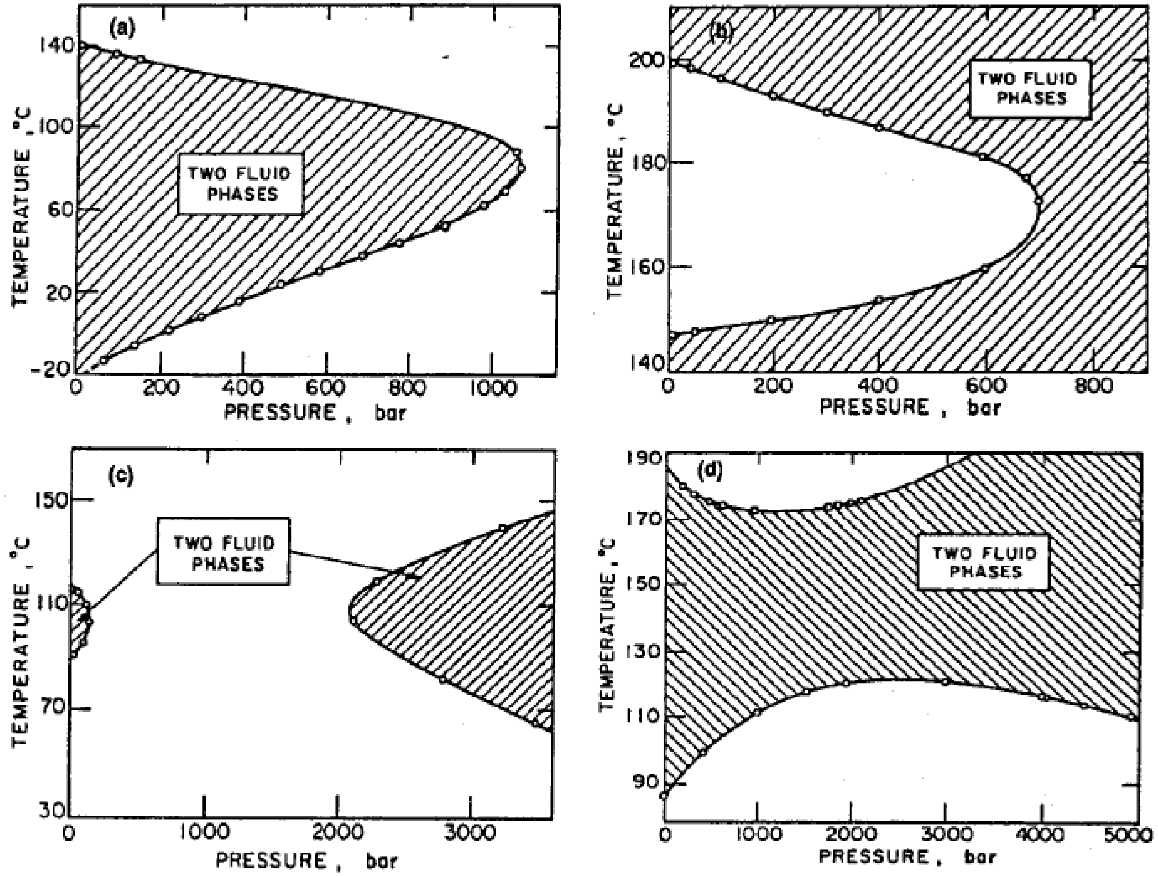

Figure 12-12 Liquid-liquid phase behavior for different binary mixtures (Timmermans, 1923; Schneider, 1966). Lower and upper consolute temperatures as functions of pressure for: (a) methyl ethyl ketone/water; (b) triphenylmethane/sulfur; (c) 2-methylpyridine/deuterium oxide; (d) 4-methylpiperidine/water.

12.3 Liquid-Liquid and Gas-Gas Equilibria

Liquid-Liquid Equilibria

- Figure 12-13 shows experimental results, liquid-liquid equilibria system.
- In this case, rising pressure increases the size of the two-phase region; in other words, rising pressure is unfavorable for miscibility.

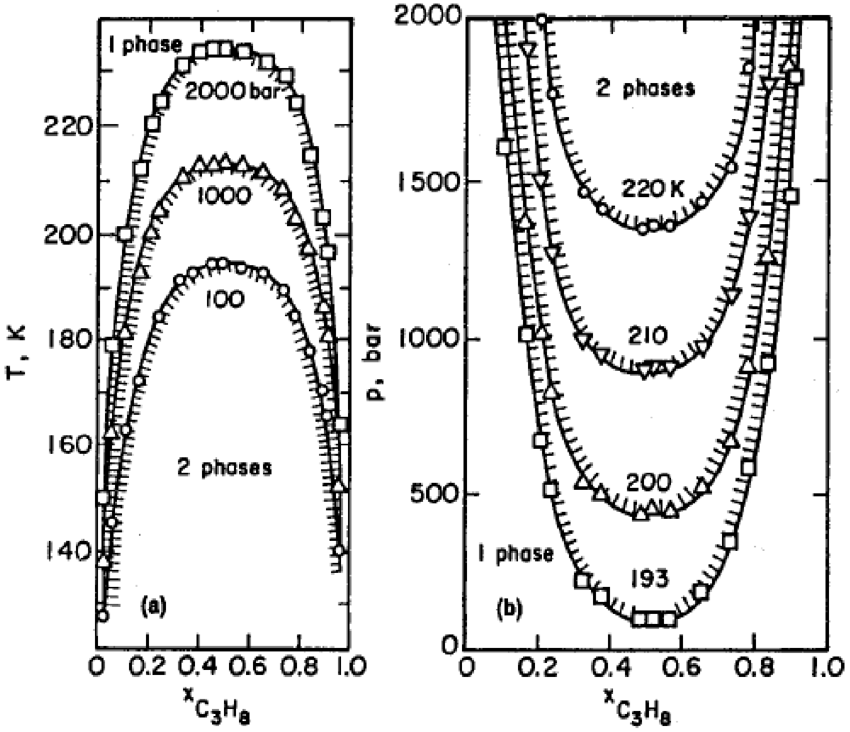

Figure 12-13 Pressure (a) and temperature (b) dependence of liquid-liquid equilibria in the system carbon tetrafluoride/propane (Jeschke and Schneider, 1982).

- Two liquids are misible in all proportions if $\triangle_{\text{mix}}g$, the molar Gibbs energy of mixing at constant temperature and pressure,

$$\Delta_{\text{mix}}g < 0 \tag{12-2}$$

and

$$\left(\frac{\partial^2 \Delta_{\text{mix}}g}{\partial x^2}\right)_{T,x} > 0 \tag{12-3}$$

for all x, because $\triangle_{\text{mix}}g$ is a function of pressure.

- The effect of pressure on miscibility in binary liquid mixtures is closely connected with the volume change on mixing, as indicated

$$\left(\frac{\partial \Delta_{\text{mix}}g}{\partial P}\right)_{T,x} = \Delta_{\text{mix}}v \tag{12-4}$$

where $\triangle_{\text{mix}}v$ is the volume change on mixing at constant temperature and pressure.

- To fix idea, consider a binary liquid mixture that at normal pressure is completely miscible and whose isothermal Gibbs energy of mixing is given by curve a in Figure 12-14

- Suppose that for this system $\triangle_{mix}v$ is positive; an increase in pressure raises $\triangle_{mix}g$, and at some higher pressure the vaiation of $\triangle_{mix}g$ with x_1 may be given by curve b.

- As indicated in Figure 12-14, $\triangle_{mix}g$ at the high pressure no longer satisfies Eq. (12-3) and the liquid mixture now has a miscibility gap in the composition interval $x_1' < x_1 < x_1''$.

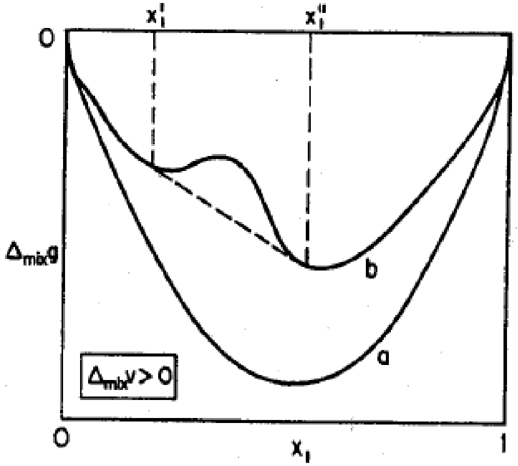

Figure 12-14 Effect of pressure on miscibility: *a* - low pressure, no immiscibility; *b* - high pressure, immiscible for $x_1' < x_1 < x_1''$.

- For contrast, consider also a binary liquid mixture that at normal pressures is in completely miscible as shown by curve a in Figure 12-15.

- If $\triangle_{\mathrm{mix}}v$ for this system is negative, then an increase in pressure lowers $\triangle_{\mathrm{mix}}g$ and at some high pressure the variation of $\triangle_{\mathrm{mix}}g$ with x_1 may be given by curve b, indicating complete miscibility.

- It follows from these simple considerations that the qualitative effect of pressure on phase stability of binary liquid mixtures depends on the magnitude and sign of the volume change of mixing.

- To carry out quantitative calculations at some fixed temperature, it is necessary to have information on the variation of $\triangle_{\mathrm{mix}}v$ with x and P in addition to information on the variation of $\triangle_{\mathrm{mix}}g$ with x at a single pressure.

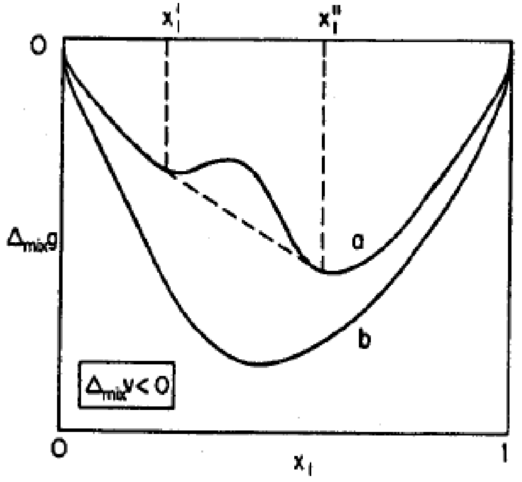

Figure 12-15 Effect of pressure on miscibility: *a* - low pressure, immiscible for $x_1' < x_1 < x_1''$; *b* - high pressure, no immiscibility.

- To illustrate, we consider a simple, symmetric binary mixture at some fixed temperature and 1 bar pressuer. For this liquid mixture, we assume that

$$\Delta_{\text{mix}} g = RT(x_1 \ln x_1 + x_2 \ln x_2) + Ax_1x_2 \qquad (12\text{-}5)$$

$$\Delta_{\text{mix}} v = Bx_1x_2 \qquad (12\text{-}6)$$

where A and B are experimentally determined constants. Further, we assume that the liquid mixture is incompressible for all values of *x*; i.e., we assuem that B is independent of pressure. At any pressue P, we have for $\triangle_{\text{mix}} g$,

$$\Delta_{\text{mix}} g = RT(x_1 \ln x_1 + x_2 \ln x_2) + \left[A + B(P-1)\right]x_1x_2 \qquad (12\text{-}7)$$

Substituting Eq. (12-7) into Eq. (12-3), we find that the mixture is partially immiscible when

$$\frac{A + B(P-1)}{RT} > 2 \qquad (12\text{-}8)$$

if A/RT < 2 and B > 0, then there is a certain pressure P (larger than 1 bar) where immiscibility is sinduced.

if A/RT > 2 and B < 0, then there is a certain pressure P (larger than 1 bar) where complete miscibility is attained.

- When two liquid phases exist,

$$f_1^{\alpha} = f_1^{\beta} \qquad (12\text{-}9)$$

$$f_2^{\alpha} = f_2^{\beta} \qquad (12\text{-}10)$$

- If the same standard-state fugacities are used in both phases, Eqs. (12-9) and (12-10) can be rewritten using activity coefficient γ:

$$(\gamma_1 x_1)^\alpha = (\gamma_1 x_1)^\beta \qquad (12\text{-}11)$$

$$(\gamma_2 x_2)^\alpha = (\gamma_2 x_2)^\beta \qquad (12\text{-}12)$$

- For the simple mixture described by Eqs. (12-5) and (12-6), we can calculate activity coefficients as discussed in Chapter 6; we substitute into Eqs. (12-11) and (12-12) and we then obtain

$$x_1^\alpha \exp\left[\frac{[A+B(P-1)](1-x_1^\alpha)^2}{RT}\right] = x_1^\beta \exp\left[\frac{[A+B(P-1)](1-x_1^\beta)^2}{RT}\right] \qquad (12\text{-}13)$$

$$x_2^\alpha \exp\left[\frac{[A+B(P-1)](1-x_2^\alpha)^2}{RT}\right] = x_2^\beta \exp\left[\frac{[A+B(P-1)](1-x_2^\beta)^2}{RT}\right] \qquad (12\text{-}14)$$

- Simultaneous solution of these equilibrium relations gives the coexistence curve for the two-phase system as a function of pressrue.

- Whilie gas-gas equilirbria are rare, liquid-liquid equilibira are common; as briefly discussed in Sec. 6.13, critical phenomena can exist in liquid-liquid system as well as in liquid-vapor systems.

- In a binary system the gas-liquid critical temperature depends on pressure, as illustrated in Figure 12-3. Similarly, in a binary system with limited liquid-phase miscibility, the liquid-liquid critical temperature also depends on pressure as shown in Figure 12-13.

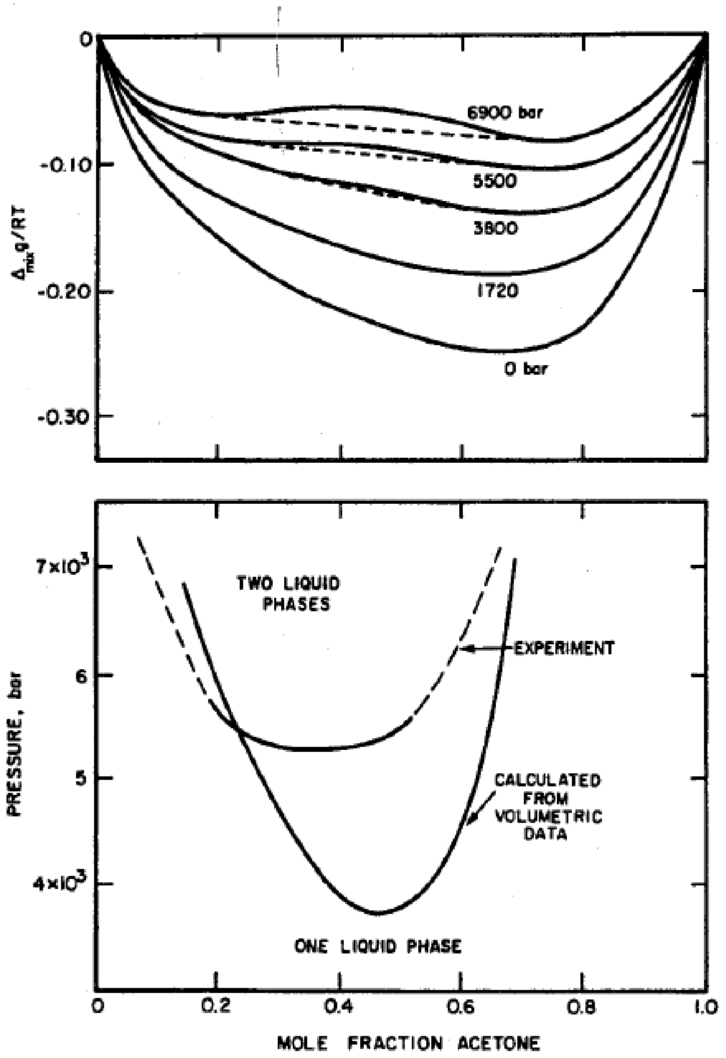

Figure 12-16 Liquid-liquid equilibria for a system completely miscible at normal pressure (Winnick and Powers, 1966). Calculated and observed behavior of the acetone/carbon disulfide system at 0°C.

- To obtain a useful equation for calculating the effect of pressure on critical solution temperature T^c, some properties are measure, others need not be, because they can be calculated.

- Sometimes, however, the quantity to be calculated requires experimental data that cannot easily be measured. In that event, it is sometimes possible to use instead other measured properties that are more readily availble.

- The effect of pressure P on critical solution temperature T^c is expressed by,

$$\frac{dT^c}{dP} = T^c \left[\frac{(\partial^2 v / \partial x^2)_{T,P}}{(\partial^2 h / \partial x^2)_{T,P}} \right]_{x_c} \qquad (12\text{-}15)$$

where v is the molar volume and h is the molar enthalpy, both at mole fraction x.

- Equation (12-15) is not useful because it is difficult to measure the second derivatives of v and h with respect to x. Further, both of these derivatives vanish at the critical point; therefor, Eq. (12-15) must be rewritten

$$\frac{dT^c}{dP} = \lim_{\substack{T \to T_c \\ x \to x_c}} \left[\frac{T(\partial^2 v / \partial x^2)_{T,P}}{(\partial^2 h / \partial x^2)_{T,P}} \right] \qquad (12\text{-}16)$$

- It would be easier to measure dT^c/dP directly. Neverthleless, Eq. (12-16) suggests an approximation, reasonable for simple mixtures, that allows us to use experimentally available quantities to estimate dT^c/dP. This approximation is a similarity hypothesis: we assume that v and h, plotted against x, show similar shapes. That is, we assume that the molar excess volume v^E and the molare excess enthalpy h^E depend on x and T according to

$$v^E = v_c^E F(x,T) \qquad (12\text{-}17)$$

$$h^E = h_c^E F(x,T) \qquad (12\text{-}18)$$

where F(x,T) is an arbitrary function of mole fraction x and temperature T. This assumption, substituted into Eq. (12-16), gives

$$\frac{dT^c}{dP} \approx \frac{T^c v_c^E}{h_c^E} \qquad (12\text{-}19)$$

where v_c^E and h_c^E are the molar excess volume and the molar excess enthalpy at critical composition x_c and critical solution temperature T_c.

Because v_c^E and h_c^E are not strongly sensitive to T and x.

- Tabe 12-2 shows a test of Eq. (12-19). Experimental results for v_c^E and h_c^E are compared with those for dT^c/dP.

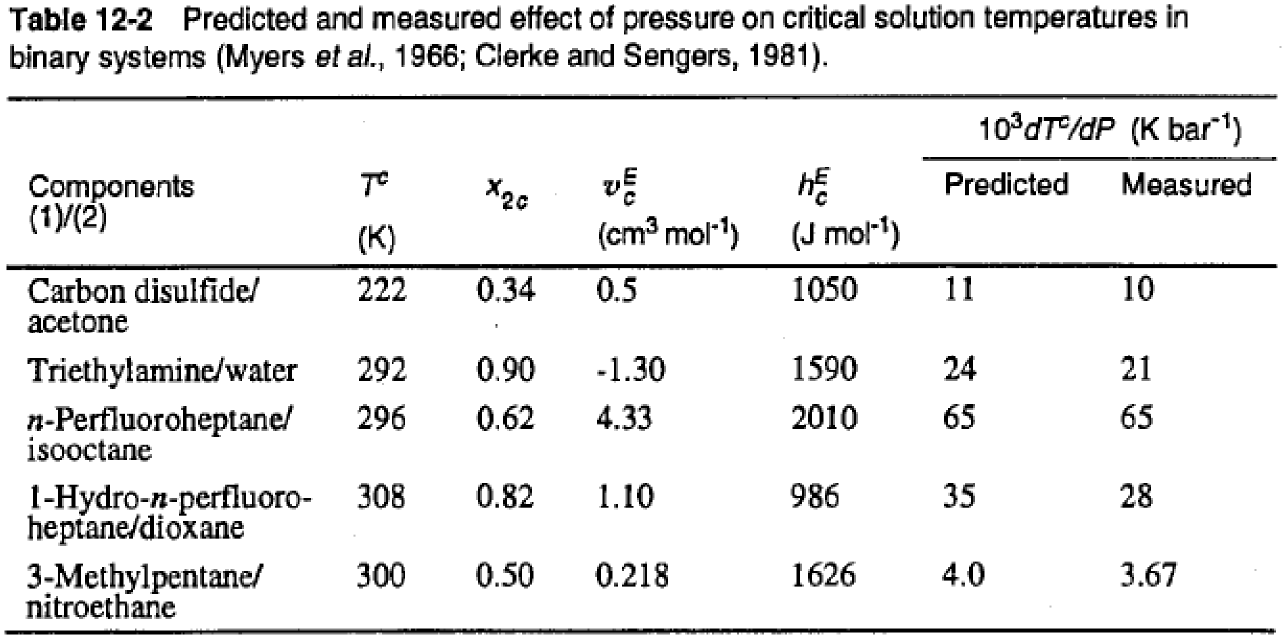

Table 12-2 Predicted and measured effect of pressure on critical solution temperatures in binary systems (Myers *et al.*, 1966; Clerke and Sengers, 1981).

Components (1)/(2)	T^c (K)	x_{2c}	v_c^E (cm^3 mol^{-1})	h_c^E (J mol^{-1})	$10^3 dT^c/dP$ (K bar^{-1})	
					Predicted	Measured
Carbon disulfide/ acetone	222	0.34	0.5	1050	11	10
Triethylamine/water	292	0.90	-1.30	1590	24	21
n-Perfluoroheptane/ isooctane	296	0.62	4.33	2010	65	65
1-Hydro-*n*-perfluoro-heptane/dioxane	308	0.82	1.10	986	35	28
3-Methylpentane/ nitroethane	300	0.50	0.218	1626	4.0	3.67

- Consider a binary liquid mixture of components 1 and 3; to be consistent with previous notation, we reserve subscript 2 for the gaseous component.

- Components 1 and 3 are completely miscible at room temperature, as indicated by the lower curve in Figure 12-17.

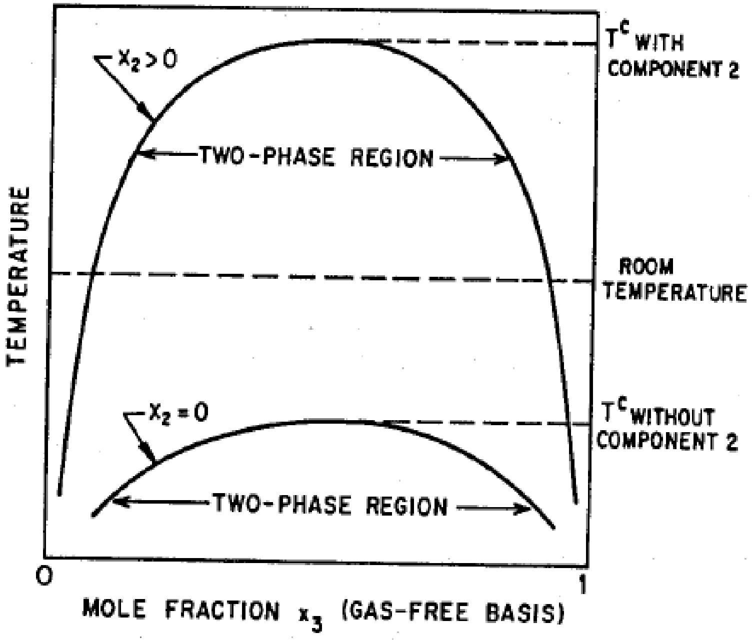

Figure 12-17 Effect of gaseous component (2) on mutual solubility of liquids (1) and (3).

- Suppose now that we dissolve a small amount of component 2 in the binary mixture.

- Prigogine assumed that for any binary pair that can be formed from the three components 1, 2, and 3, the excess Gibbs energy is

$$g_{ij}^E = \alpha_{ij} x_i x_j \quad (i, j = 1,2;\ 1,3;\ \text{or } 2,3) \tag{12-20}$$

where α_{ij} is an empirical (Margules) coefficient determined by the properties of the i-j binary.

- Prigogine has shown that, upon adding a small amount of component 2, the rate of change in critical temperature is given by

$$\frac{\partial T^c}{\partial x_2} = -\frac{1}{2R}\frac{(\alpha_{13} - \alpha_{12} + \alpha_{23})(\alpha_{13} - \alpha_{23} + \alpha_{12})}{\alpha_{12}} \qquad (\text{for } x_2 << 1) \tag{12-21}$$

- On the common case where all three binaries exhibit positive deviations from Raoult's law, i.e., $\alpha_{ij} > 0$ for all i-j pairs.

- If T^c for the 1-3 binary is far below room temperature, then that binary is only moderately nonideal and α_{13} is small.

- A gas that forms a highly nonideal solution with one of the liquid components (say component 3) while it forms with the other component (component 1) a solution that is only modestly nonideal. In that event,

$$\alpha_{23} >> \alpha_{12} \tag{12-22}$$

and

$$\alpha_{23} >> \alpha_{13} \tag{12-23}$$

- Equations (12-21), (12-22), and (12-23) indicate that under the comditions described, $\partial T^c/\partial x^2$ is both large and positive, as desired; i.e., dissolution of a small amount of component 2 in the 1-3 mixture raises the critical solution temperature.

- From Prigogine's analysis we conclude that if component 2 is properly chosen, it can induce binary miscible mixtures of components 1 and 3 to split at room temperature into two liquid phases having different compositions.

Gas-Gas Equilibria

- Thermodynamic analysis of incomplete miscibility in liquid mixtures at high pressures [Eqs. (12-2), (12-3), and (12-4)] can also be applied to gaseous mixtures at high pressures.

- Figure 12-18 shows some experimental results for the helium/xenon system. As described in Sec. 12.2, the mixture helium/xenon is of type 3 and forms gas-gas equilibria of the first kind.

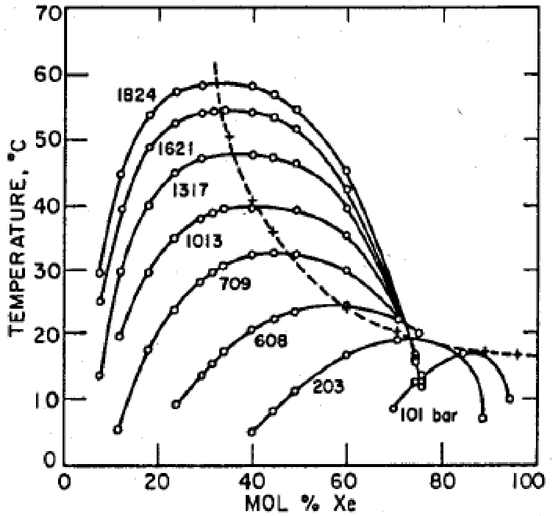

Figure 12-18 Gas-gas equilibria in the helium/xenon system (de Swaan Arons and Diepen, 1966).

- Equations of state provide a logical model for gas-gas equilibrium calculations. That is, at least in principle, it is possible to compute phase diagrams such as those shown in Figure 12-6.

- Using conventional mixing rules, phase diagrams as in Figure 12-6 can be qualitatively predicted.

- Quantitative calculation of critical lines requires not only a good equation of state for mixtures, but also sophisticated computing techniques.

- Suppose we have a binary gaseous mixture containing components 1 and 2, such that critical temperature T_{c2} is larger than T_{c1}.

- Assume that the properties of the mixture are given by the original van der Waals equation with constant b given by a linear function and constant a by a quadratic function of mole fraction.

- What conditions must be met by pure-component constants a and b and by binary constant a_{12} to produce gas-gas equilibria?

$$b_1 \geq 0.42 b_2 \tag{12-24}$$

and that

$$\frac{1}{2}(a_1 + a_2) - a_{12} > \frac{8}{27} a_2 \tag{12-25}$$

- Because component 2 is the heavier component, Eq. (12-24) tells us that gas-gas equilibria near T_{c2} are unlikely if there is a very large difference in molecular sizes, i.e., b_1 can be smaller than b_2 but not very much smaller.

- Equation (12-25) tells us that the attractive forces between unlike molecules (given by a_{12}) must be appreciably lower than those calculated by the arithmetic mean of a_1 and a_2. These conclusions are consistent with our intuitive ideas about mixtures.

- Equation (12-25) also is easy to understand. It says that for partial miscibility, the forces of attraction between unlike molecules must be weak; if molecules 1 and 2 do not like each other, they have little tendency to mix, but prefer to stay with neighbors identical to themselves.

- If we assume that for nonpolar systems, $a_{12}=(a_1 a_2)^{1/2}$, Eq. (12-25) reduces to

$$a_1 < 0.053 a_2 \tag{12-26}$$

- In other words, the intermolecular force parameter a_1 must be less than about 5% of parameter a_2.

12.4 Thermodynamic Analysis

- For any component *i*, the fugacity of *i* must be the same in all equilibrated phases.

- However, this equilibrium relation is of no use until we can relate the fugacity of a component to directly measurable properties.

- For any component i in a system containing m components, the total differential of the logarithm of the fugacity f_i is

$$d\ln f_i = \left(\frac{\partial \ln f_i}{\partial T}\right)_{P,x} dT + \left(\frac{\partial \ln f_i}{\partial P}\right)_{T,x} dP + \sum_{j=1}^{m-1}\left(\frac{\partial \ln f_i}{\partial x_j}\right)_{T,P,x_k} dx_j \qquad (12\text{-}27)$$

$$k = 1,\ldots,j-1,j+1,\ldots,m-1$$

- The first tem can be related to the partial molar enthalpy and the second to the partial molar volume; the third term can be related to the Gibbs energy and that, in turn, can be described by a solution model or an equation of state.

- In high pressure work, it is important to give particular attention to the second coefficient that tells us how phase behavior is affected by pressure.

- When analyzing experimental data, it is difficult to isolate the effect of pressure because, a change in the pressure is accompanied by a simultaneous change in either the temperature or the composition, or both.

- Such simultaneous changes is given by experimental results in Figure 12-19.

- Line A; the melting temperatures rises with pressure.

- Line B; these results are similar to those for pure argon, and again the melting temperature rises with increasing pressure.

- Line C; the melting temperature now falls with rising pressure.

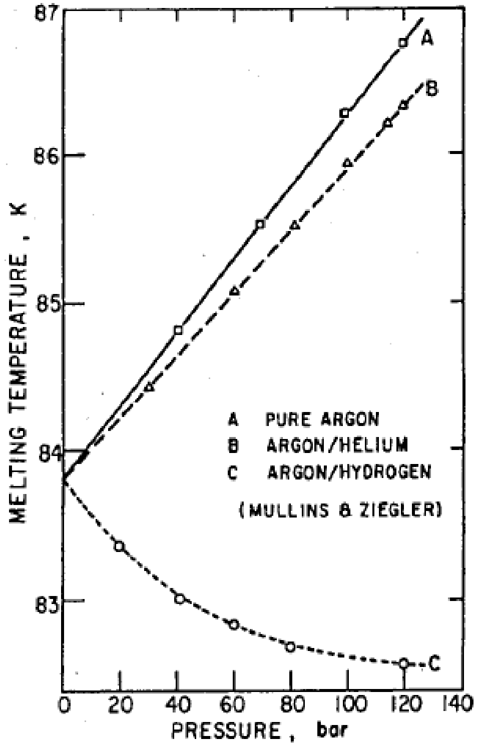

Figure 12-19 Effect of pressure on melting temperature of argon. Qualitative difference between lines *B* and *C* is due to effect of composition on the liquid-phase fugacity of argon.

- We merely with to emphasize that the fugacity of a component is determined by the three variables temperature, pressure, and composition; that in a typical experimental situation these influences operate in concert; and that whatever success we may expect in explaining the behavior of a multicomponent, multiphase system is determined directly by the extent of our knowledge of the three coefficients given in Equation (12-27).

- At present we know least about the first coefficient, rigorously related to enthalpy by

$$\left(\frac{\partial \ln f_i}{\partial T}\right)_{P,x} = -\frac{\bar{h}_i - h_i^+}{RT^2} \qquad \text{(12-28)[12]}$$

where h_i^- is the partial molar enthalpy of i and h_i^+ is the molar enthalpy of i in the ideal-gas state at the same temperature.

- So little is known about enthalpies of fluid mixtures at high pressures. As a result, the best procedure for most cases is to analyze experimental phase-equilibrium data as a function of pressure and composition along an isotherm, and to allow any empirical parameters obtained from such analysis to vary with temperature as dictated by the experimental results.

- While formal thermodynamic analysis is equally useful for predicting the effect of pressure, temperature, or composition on phase behavior, it is the effect of pressure that is often simplest to understand because it is directly related to volumetric data through the fundamental relation for molar Gibbs energy g.

$$\left(\frac{\partial g}{\partial P}\right)_{T,x} = v \qquad \text{(12-29)}$$

that, in turn, leads to

$$\left(\frac{\partial \ln f_i}{\partial P}\right)_{T,x} = \frac{\bar{v}_i}{RT} \qquad \text{(12-30)}$$

- To illustrate, consider the solubility of nitrogen in water at 18℃. Let subscript 2 stand for nitrogen. At equilibrium,

$$f_2^V = f_2^L \qquad \text{(12-31)}$$

Taking logarithms and total differentials, Eq. (12-31) becomes

$$d\ln f_2^V = d\ln f_2^L \qquad \text{(12-32)}$$

At constant temperature,

$$d\ln f_2^V = \left(\frac{\partial \ln f_2^V}{\partial P}\right)_{y_2} dP + \left(\frac{\partial \ln f_2^V}{\partial \ln y_2}\right)_P d\ln y_2 \qquad (12\text{-}33)$$

and

$$d\ln f_2^L = \left(\frac{\partial \ln f_2^L}{\partial P}\right)_{x_2} dP + \left(\frac{\partial \ln f_2^L}{\partial \ln x_2}\right)_P d\ln x_2 \qquad (12\text{-}34)$$

Because nitrogen is sparingly soluble in water at 18℃, Henry's law holds; therefore, at constant temperature,

$$\left(\frac{\partial \ln f_2^L}{\partial \ln x_2}\right)_P = 1 \qquad (12\text{-}35)$$

At 18℃, the volatility of water is very low: $y_2 \doteqdot 1$, and therefore the last term in Equation (12-33) can be neglected.

Substituting Eqs. (12-33), (12-34) and (12-35) into Eq.(12-32), we obtain at constant temperature,

$$\frac{d\ln x_2}{dP} = \left(\frac{d\ln f_2^V}{dP}\right)_{y_2} - \left(\frac{d\ln f_2^L}{dP}\right)_{x_2} = \frac{\bar{v}_2^V - \bar{v}_2^L}{RT} \qquad (12\text{-}36)$$

Because $y_2 \doteqdot 1$, we can set the vapor-phase partial molar volume of nitrogen equal to the molar volume of pure gaseous nitrogen, $V_{N2}{}^G$ and solubility $x_2 << 1$, we can set

$$\bar{v}_2^L = \bar{v}_2^\infty \qquad (12\text{-}37)$$

While V_{N2}^{G} is a strong function of pressure, V_2^{∞} is essentially independent of pressure in a solvent far below its critical temperature.

- Two variables are shown as a function of pressure in the lower part of Figure 12-20.

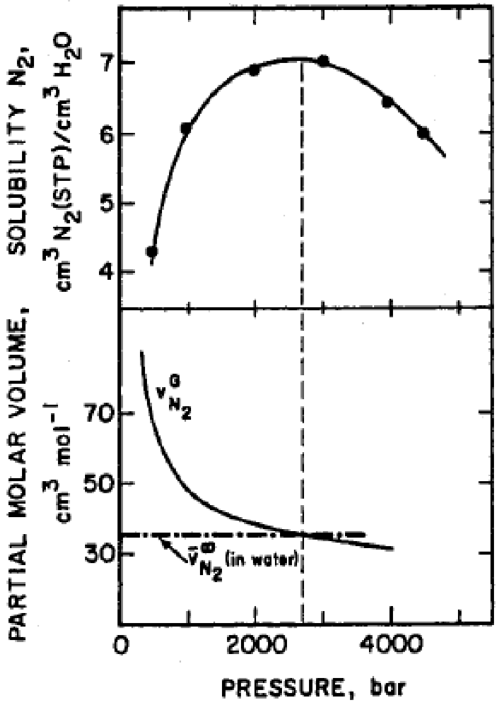

Figure 12-20 Solubility of nitrogen in water at 18°C. Calculation of maximum solubility according to the Krichevsky-Kasarnovsky equation.

- It is difficult to measure partial molar volumes and unfortunately many experimental studies of high-pressure vapor-liquid equilibria report no volumetric data at all; more often than not, experimental measurements are confined to total pressure, temperature, and phase compositions.

$$\bar{v}_1 = v^s - x_2\left[\left(\frac{\partial v^s}{\partial x_2}\right)_T + v^s \kappa_T \left(\frac{\partial P}{\partial x_2}\right)_T\right] \qquad (12\text{-}38)$$

$$\bar{v}_2 = v^s + x_1\left[\left(\frac{\partial v^s}{\partial x_2}\right)_T + v^s \kappa_T \left(\frac{\partial P}{\partial x_2}\right)_T\right] \qquad (12\text{-}39)$$

where compressibility κ_T is defined by

$$\kappa_T \equiv -\frac{1}{v^s}\left(\frac{\partial v^s}{\partial P}\right)_{T,x} \qquad (12\text{-}40)$$

- For dilute solutions, the accuracy of the partial molar volume is usually not high. A survey by Lyckman (1965) established the rough correlation shown in Figure 12-21.

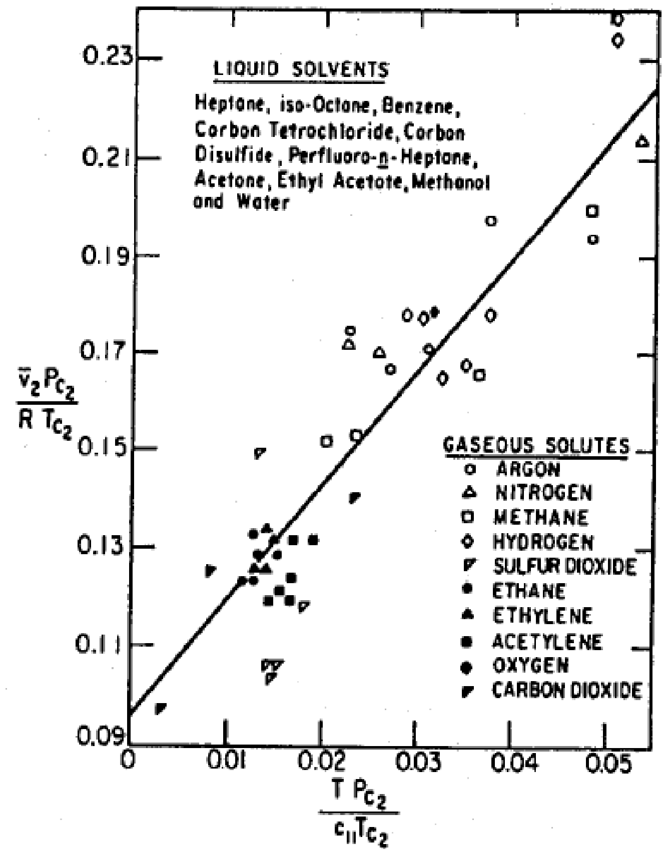

Figure 12-21 Partial molar volumes of gases in dilute liquid solutions.

- For expanded solvents, the partial molar bolume of the solute tends to be much larger than that suggested by the correlation as indicated in Figure 12-22.

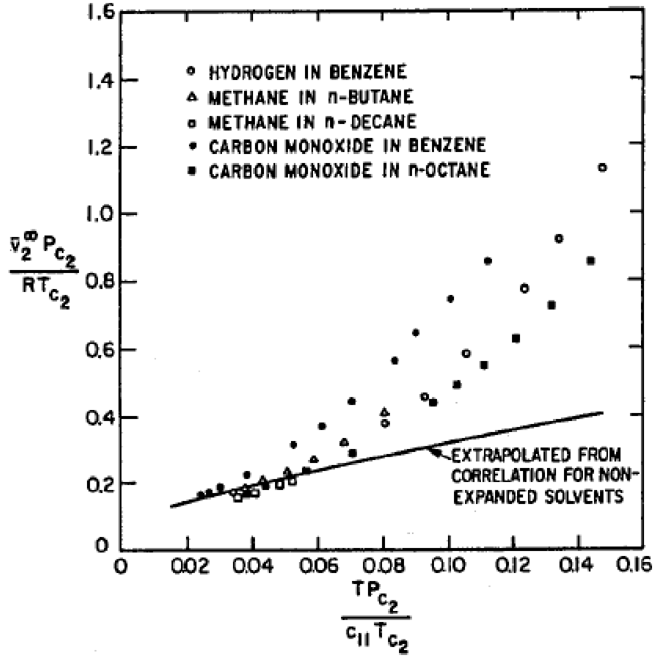

Figure 12-22 Partial molar volumes of gaseous solutes at infinite dilution in expanded solvents.

- If we can write an equation of state for liquid mixtures, we can then calculate partial molar volumes directly by differentiation. For a pressure-explicit equation, the most convenient procedure is to use the exact relation

$$\bar{v}_i \equiv -\frac{(\partial P / \partial n_i)_{T,V,n_j}}{(\partial P / \partial V)_{T,\ \text{all}\ n}} \tag{12-41}$$

where V is the total volume of the mixture containing n_1 moles of component 1, etc.

12.5 Supercritical-Fluid Extraction

This solubility can become surprisingly large when the compressed gas is near its critical point, leading to a separation operation called supercritical fluid extraction.

Consider the solubility of a heavy component(2) in a dense gas (1) at temperature T and pressure P. For simplicity, let component 2 be a solid such that the solubility of component 1 in the solid phase is negligible. The equation of equilibrium is

$$f^{s}_{\text{pure }2} = \varphi_2 y_2 P \qquad (12\text{-}42)$$

Where y is the mole fraction in the vapor phase and φ is the vapor-phase fugacity coefficient.
At gas-phase densities approaching the critical, solubility y2 is sensitive to small changes in T and P because, in the critical region, these have a large effect on the gas phase density. This sensitivity has applications in separation technology (supercritical extraction), where solvent recovery is an important economic consideration.

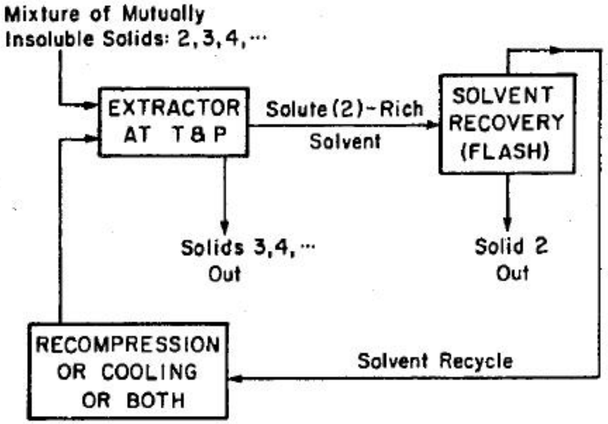

Figure 12-23 Idealized application of supercritical extraction. Temperature *T* and pressure *P* are slightly above the solvent's critical. In the recovery step, a small drop in *P* (or small rise in *T*) significantly lowers the solubility of solid 2 in the gaseous solvent. (In this idealized example, the solvent is totally selective for solid 2.)

Figure 12-23 shows a schematic diagram of a particularly simple supercritical-extraction separation process. Extractions with supercritical fluids are potentially useful in many industries, in particular for extraction of bioactive substances from natural products (for a review, see King, 1993 and Rizvi, 1994).

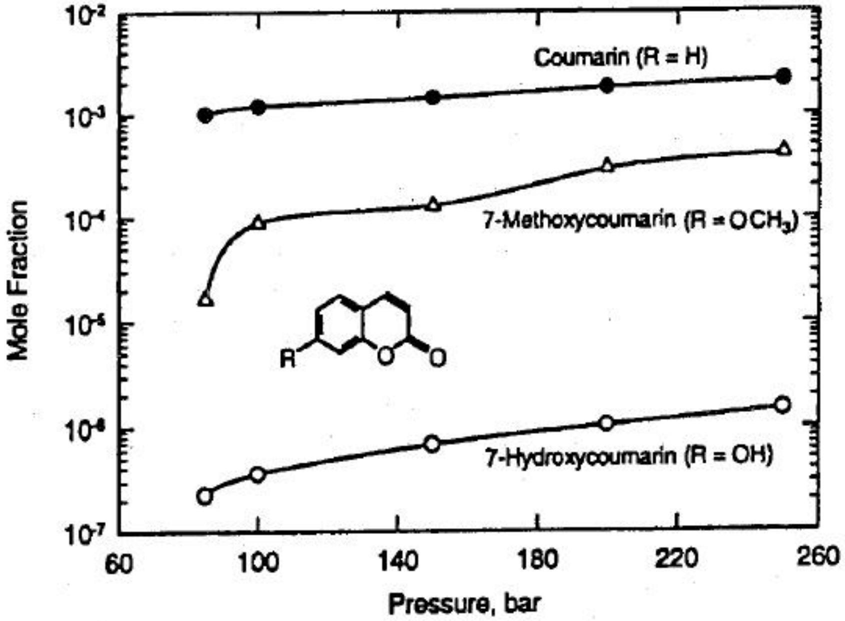

Figure 12-24 Solubility of coumarin, 7-methoxycoumarin and 7-hydroxycoumarin in supercritical CO_2 at 308.15 K (Yoo *et al.*, 1997). Lines are best fit of experimental data.

Figure 12-24 compares solubilities at 308.15K of coumarin and its methoxy-group and hydroxyl-group derivatives in supercritical CO2. As Fig 12-24 shows coumarin exhibits the highest solubility in CO2. This large solubility difference is required for the feasibility of any supercritical-fluid-base extraction process.

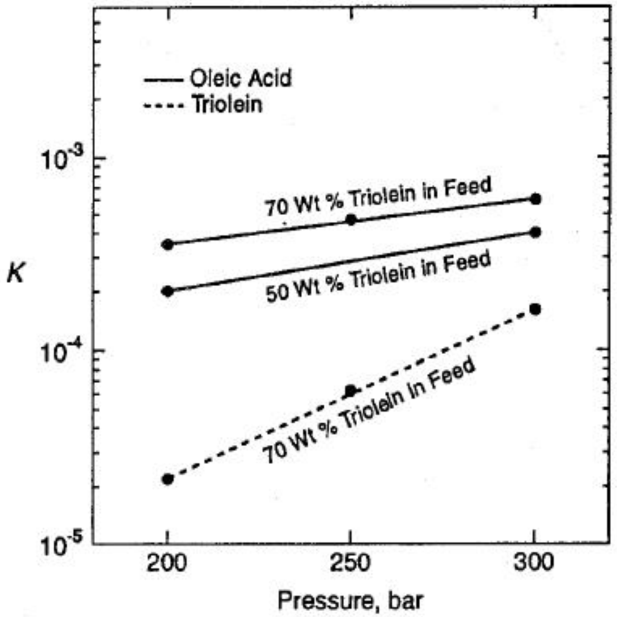

Figure 12-25 *K* factors (Bharath *et al.*, 1992) as a function of pressure (for feeds of 50 weight % and 70 weight % of triolein, CO_2-free basis) for oleic acid (——) and triolein (– – – –) obtained from vapor-liquid-equilibrium data with supercritical CO_2 at 40°C.

Figure 12-25 presents an illustration of a practical application of supercritical fluid solvents in the oleochemical industry. This figure shows distribution coefficients (K factors) of oleic acid and triolein in supercritical carbon dioxide at 40℃.K for oleic acid is ten times larger than that of triolein, suggesting that extraction with supercritical CO2 can provide an alternative to conventional fractionation processes such as solvent extraction and low pressure distillation.

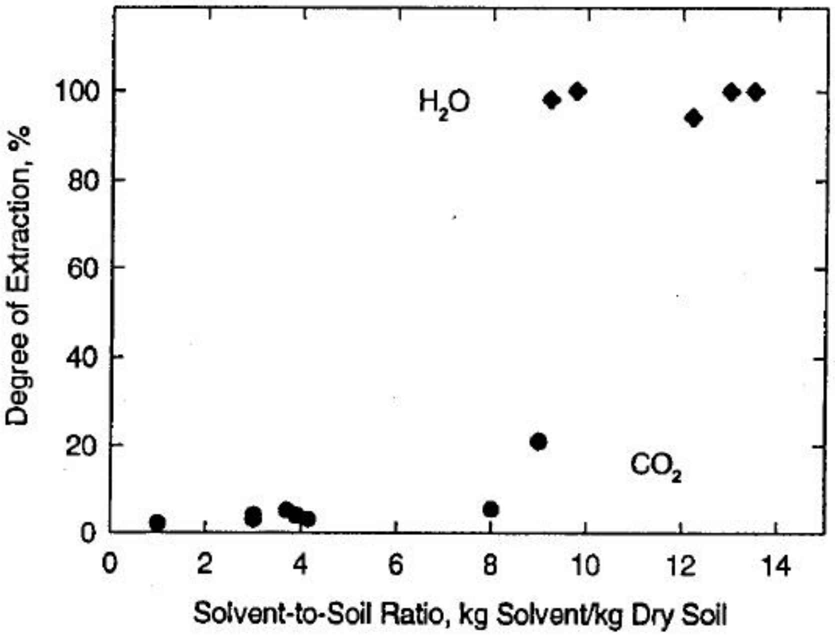

Figure 12-26 Extraction of hydrocarbons from soil with supercritical CO_2 and H_2O as a function of solvent-to-soil ratio. ◆ : H_2O at 653 K and 25 MPa; ●: CO_2 at 353 K and 20 MPa. The critical temperature of CO_2 is 304 K and that of water is 647 K.

Figure 12-26 shows that supercritical water (at 653K and 25MPa) removes virtually all the contaminants from the soil. However, supercritical CO2 achieves no more than 21% of extraction, because of the lower operation temperature.

In modeling the phase behavior of natural products such as those indicated in Fig 12-24, and Fig 12-25, there is an additional difficulty : due to the complex nature of most natural products, basic physical properties and constant are not available.

As indicated by Eq. (12-42), when pressure and temperature are held constant, solubility y2 is inversely proportional to φ2. The advantage of supercritical extraction follows from the sensitivity of φ2 to pressure when the solvent′s density is near its critical.

$$f^{s}_{\text{pure }2} = \varphi_2 y_2 P \tag{12-42}$$

The effect of pressure P on fugacity coefficient φ2 is directly related to the partial molar volme :

$$\left(\frac{\partial \ln \varphi_2}{\partial P}\right)_{T,y} = \frac{\overline{v}_2}{RT} - \frac{1}{P} \tag{12-43}$$

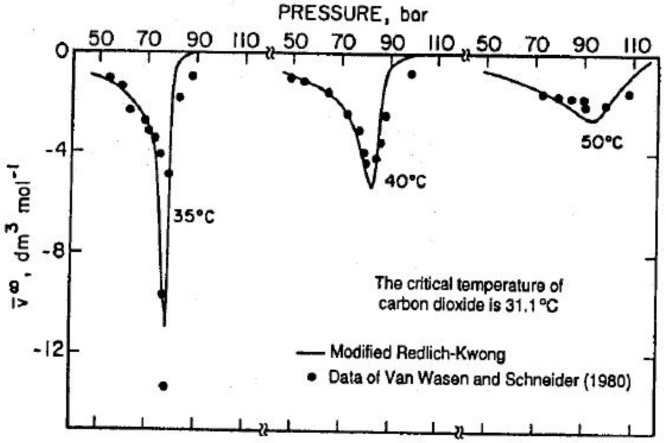

Figure 12-27 Partial molar volumes of naphthalene infinitely dilute in compressed carbon dioxide. Partial molar volumes are large and negative in the critical region.

Figure 12-27 and Eq. (12-43) indicate that at pressures near 78bar and at 35℃, a small decrease in pressure very much raises φ2 thereby very much reducing solubility y2. The sharp change in φ2 with pressure is the basis of efficient solute recovery in supercritical fluid extraction.

12.6 Calculation of High-Pressure Vapor-Liquid Equilibria

Consider a binary liquid mixture with mole fractions x1 and x2 at temperature T and pressure P : in equilibrium with this liquid mixture is a vapor with mole fractions y1 and y2.
The equations of equilibrium are

$$f_1^V = f_1^L \quad \text{or} \quad \varphi_1^V y_1 = \varphi_1^L x_1 \tag{12-44}$$

$$f_2^V = f_2^L \quad \text{or} \quad \varphi_2^V y_2 = \varphi_2^L x_2 \tag{12-45}$$

Where f is the fugacity and φ is the fugacity coefficient. The equilibrium ratios (K factors) are given by

$$K_1 \equiv \frac{y_1}{x_1} = \frac{\varphi_1^L}{\varphi_1^V} \tag{12-46}$$

$$K_1 \equiv \frac{y_2}{x_2} = \frac{\varphi_2^L}{\varphi_2^V} \tag{12-47}$$

12.7 Phase Equilibria from Equations of State.

In the equation-of-state method, a single equation of state is used to represent all fluid phases : for vapor-liquid equilibria, the equation is assumed to be valid for both the vapor-phase mixture and the liquid-phase mixture.

For each component i in the vapor phase,

$$\ln \varphi_i^V = \frac{1}{RT} \int_{V^V}^{\infty} \left[\left(\frac{\partial P}{\partial n_i} \right)_{T,V,n_j} - \frac{RT}{V} \right] dV - \ln \frac{PV^V}{n_T RT} \qquad (12\text{-}48)$$

Similarly, for each component i in the liquid phase,

$$\ln \varphi_i^L = \frac{1}{RT} \int_{V^L}^{\infty} \left[\left(\frac{\partial P}{\partial n_i} \right)_{T,V,n_j} - \frac{RT}{V} \right] dV - \ln \frac{PV^L}{n_T RT} \qquad (12\text{-}49)$$

Where n_i and n_T now refer to the liquid phase.

To use Eqs. (12-48) and (12-49), we require a suitable equation of state that hold for the entire range of possible mole fractions x and y at system temperature T and for the density range between 0 and $(n_T/V)^L$.

To fix ideas, consider, for example, Soave′s(1972) modification of the Redlich-Kwong equation:

$$P = \frac{RT}{v-b} - \frac{a(T)}{v(v+b)} \qquad (12\text{-}50)$$

Where a(T) depends on temperature according to

$$a(T) = a(T_c)\,\alpha(T) \qquad (12\text{-}51)$$

$$a(T_c) = 0.42748\,\frac{(RT_c)^2}{P_c} \qquad (12\text{-}52)$$

Where, for normal fluids,

$$\alpha(T) = [1 + (0.480 + 1.574\omega - 0.176\omega^2)(1 - \sqrt{T/T_c})]^2 \qquad (12\text{-}53)^{18}$$

For acentric factors $0 < w < 0.5$
Constant b is given by

$$b = 0.08664 \frac{RT_c}{P_c} \qquad (12\text{-}54)$$

as in the Redlich-Kwong equation.

One-fluid theory assumes that for the mixture we can generalize Eq. (12-50), i.e. to assume that it holds for the mixtures for both phases. The remaining task is to specify how b and a(T) depend on composition (mixing rules).

The common procedure is to write mixing rules that are quadratic in mole fraction
For a binary mixture,

$$b = z_1^2 b_{11} + 2 z_1 z_2 b_{12} + z_2^2 b_{22} \qquad (12\text{-}55)$$

$$a(T) = z_1^2 a_{11}(T) + 2 z_1 z_2 a_{12}(T) + z_2^2 a_{22}(T) \qquad (12\text{-}56)$$

Constant b_{ii} and $a_{ii}(T)$ refer to the pure-component values ; however, b_{12} and $a_{12}(T)$ are binary parameters. It is convenient to express these in the form

$$b_{12} = \frac{1}{2}(b_{11} + b_{22})(1 - c_{12}) \qquad (12\text{-}57)$$[19]

$$a_{12}(T) = [a_{11}(T) a_{22}(T)]^{1/2}(1 - k_{12}) \qquad (12\text{-}58)$$

To illustrate this method for calculating high-pressure vapor liquid equilibria, Fig. 12-28 shows results for the system methane/propane.

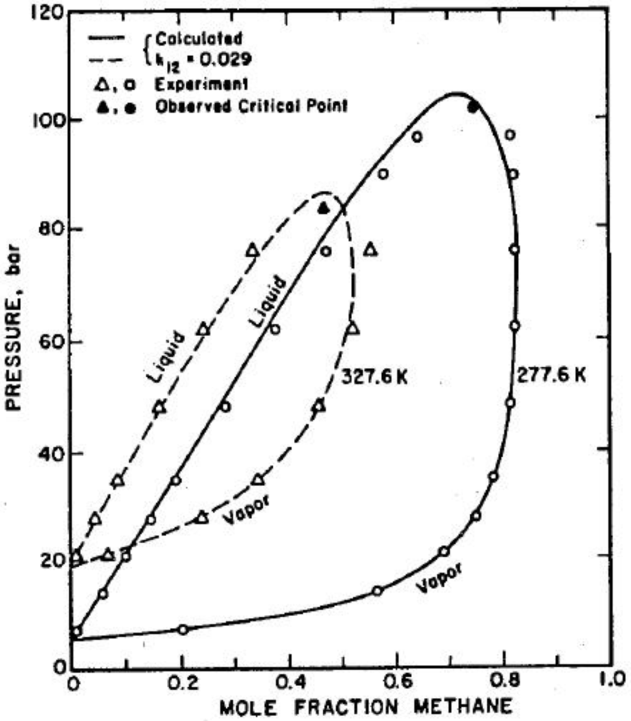

Figure 12-28 Isothermal pressure-composition diagram for methane/propane. Calculations using Redlich-Kwong-Soave equation of state. Experimental data from Reamer *et al.* (1950).

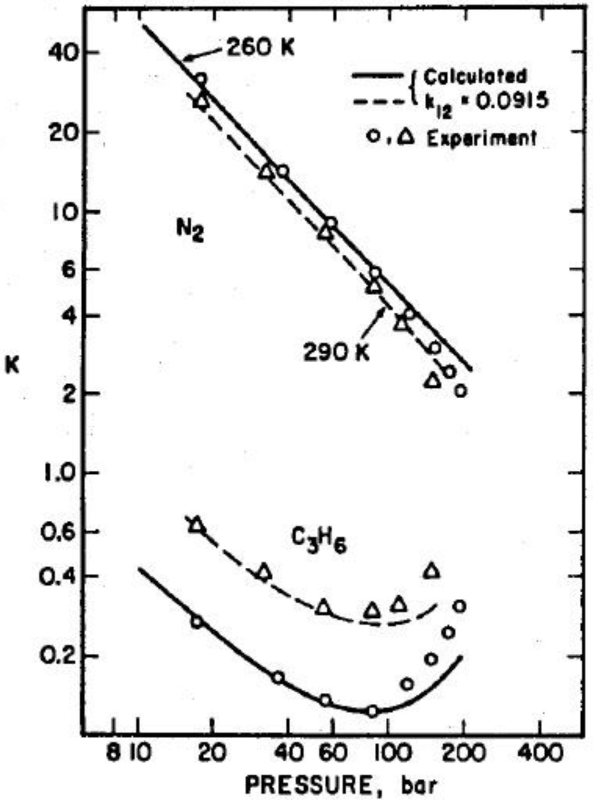

Figure 12-29 Calculated and observed (Grausø *et al.*, 1977) *K* factors for nitrogen/propylene. Calculations using Redlich-Kwong-Soave equation of state.

Figure 12-29 shows calculated K factors for nitrogen/propylene, using $c_{12} = 0$ and $k_{12} = 0.0915$.

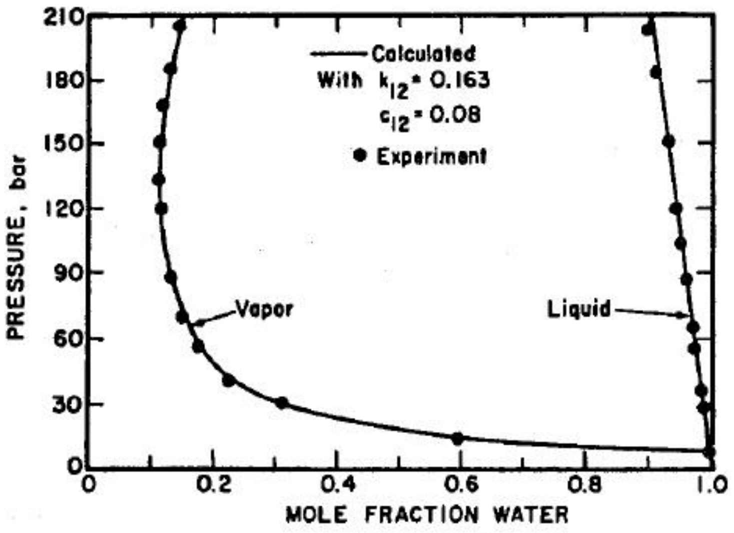

Figure 12-30 Experimental (Selleck *et al.*, 1952) and calculated (Evelein *et al.*, 1976) phase equilibria for the system hydrogen sulfide/water at 171°C.

Another illustration is given in Fig. 12-30 for the system hydrogen sulfide/water.

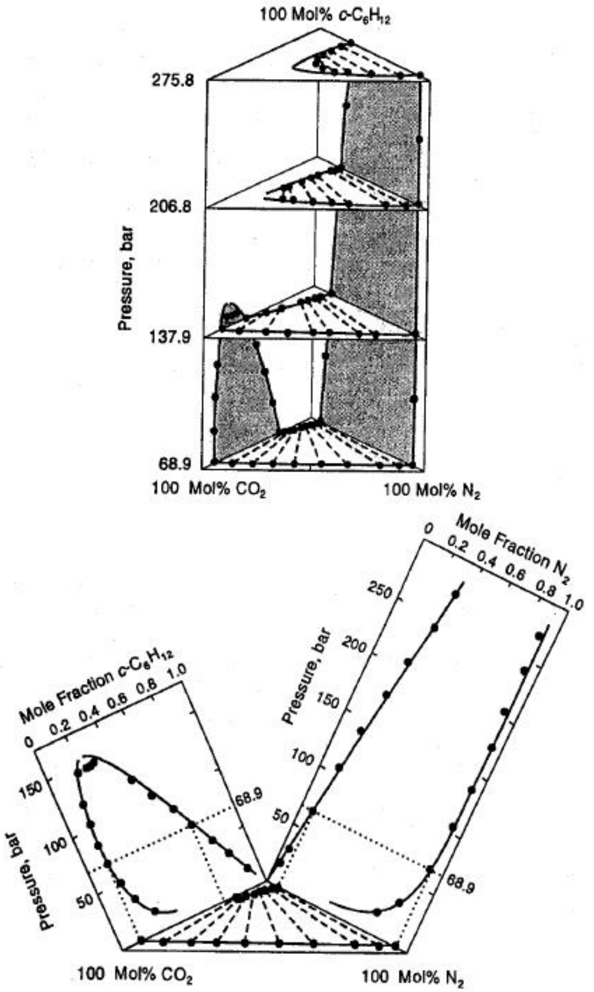

Figure 12-31 Vapor-liquid equilibria for the system $N_2/CO_2/c\text{-}C_6H_{12}$ at 410.9 K. The four triangles shown on top are isothermal-isobaric phase diagrams for the ternary mixture at 410.9 K and at the pressures indicated. At bottom, phase diagrams of the constituent binaries $CO_2/c\text{-}C_6H_{12}$ and $N_2/c\text{-}C_6H_{12}$ (also at 410.9 K) and their relation to the 68.9-bar triangular diagram. ● Experiment; —— Calculated from Peng-Robinson equation with the binary parameters listed in Table 12-3. (Shibata and Sandler, 1989).

In addition to experimental data, Fig. 12-31 shows also calculations using the Peng-Robinson equation of state :

$$P = \frac{RT}{v-b} - \frac{a(T)}{v(v+b)+b(v-b)} \qquad (12\text{-}59)$$

For a pure fluid, constant b is given by

$$b = 0.07780\frac{RT_c}{P_c} \qquad (12\text{-}60)$$

While a(T), a function of temperature, is given by

$$a(T) = a(T_c)\alpha(T) \qquad (12\text{-}61)$$

$$a(T_c) = 0.45724\frac{(RT_c)^2}{P_c} \qquad (12\text{-}62)$$

$$\alpha(T) = \left[1+\beta(1-\sqrt{T/T_c})\right]^2 \qquad (12\text{-}63)$$

Here, Tc is the critical temperature and β depends on acentric factor w according to

$\beta = 0.37464 + 1.54226w - 0.26992w^2$ (for $0 \le w \le 0.5$)

Using the conventional mixing rules for a mixture [Eqs. (12-55) and (12-56)], the fugacity coefficient for component k in a mixture is given by

$$\ln \varphi_k = \frac{b_k}{b}\left(\frac{Pv}{RT}-1\right)-\ln\frac{P(v-b)}{RT}-\frac{a}{2\sqrt{2}\,bRT}\left[\frac{2\sum_i y_i a_{ik}}{a}-\frac{b_k}{b}\right]\ln\frac{v+(1+\sqrt{2})b}{v+(1-\sqrt{2})b} \qquad (12\text{-}64)$$

The phase behavior of the ternary N_2 /CO_2 / c-C_6H_{12} system was predicted using the binary parameters k ij given in Table 12-3, determined from binary data only.

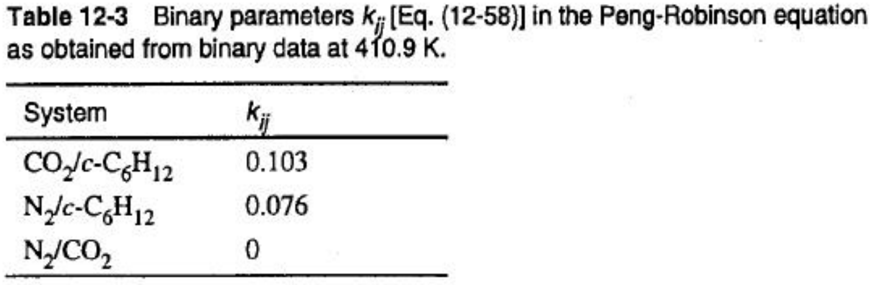

Table 12-3 Binary parameters k_{ij} [Eq. (12-58)] in the Peng-Robinson equation as obtained from binary data at 410.9 K.

System	k_{ij}
CO_2/c-C_6H_{12}	0.103
N_2/c-C_6H_{12}	0.076
N_2/CO_2	0

Figure 12-31 shows good agreement between experimental and calculated results. But, near the critical region agreement is not satisfactory. In critical region, density fluctuations contribute strongly to thermodynamic properties. These fluctuations, ignored in van der waals type equations of state, can be taken into account but the procedure for doing so is complex.

Non-Quadratic Mixing Rules

For highly non-ideal mixtures quadratic mixing rules are inadequate. Several methods have been proposed to modify the original mixing rules. In many cases the modified mixing rules include composition-dependent or density-dependent binary interaction parameters.

The Wong-Sandler model is applied to a van der waals-type equation of state with

$$b_{\mathrm{mixt}} = \frac{\sum_i \sum_j x_i x_j \left(b - \frac{a}{RT} \right)_{ij}}{1 - \frac{a_\infty^E}{CRT} - \sum_i x_i \left(\frac{a_i}{b_i RT} \right)} \qquad (12\text{-}65)$$

and

$$a_{\mathrm{mixt}} = b_{\mathrm{mixt}} \left[\sum_i x_i \frac{a_i}{b_i} + \frac{a_\infty^E (x_i)}{C} \right] \qquad (12\text{-}66)$$

Where C is a constant dependent on the equation of state. For the Peng-Robinson equation,
$C = [\ln(\sqrt{2} - 1)] / \sqrt{2} = -0.62322$

The composition-independent cross second virial coefficient $[b-a/(RT)]_{ij}$, obtained from the equation of state, is related to those of the pure components by

$$\left(b-\frac{a}{RT}\right)_{ij}=\frac{1}{2}\left[\left(b_i-\frac{a_i}{RT}\right)+\left(b_j-\frac{a_j}{RT}\right)\right](1-k_{ij}) \qquad (12\text{-}67)$$

Where kij is a binary interaction parameter for the second virial coefficient.

For the high-density limit, Wong and sandler equate the excess Helmholtz energy at infinite pressure obtained from the equation of state to that obtained from a chosen liquid phase activity coefficient model(van Laar of NRTL, etc.), using the approximation

$$g^E(T,P=1\text{ bar},x_i)\approx a^E(T,P=1\text{ bar},x_i)\approx a^E(T,\text{high pressure},x_i)\equiv a_\infty^E(T,x_i)$$

Where $a_\infty^E(T,x_i)$ is the molar excess Helmholtz energy for a fixed composition and temperature in the infinite pressure limit.

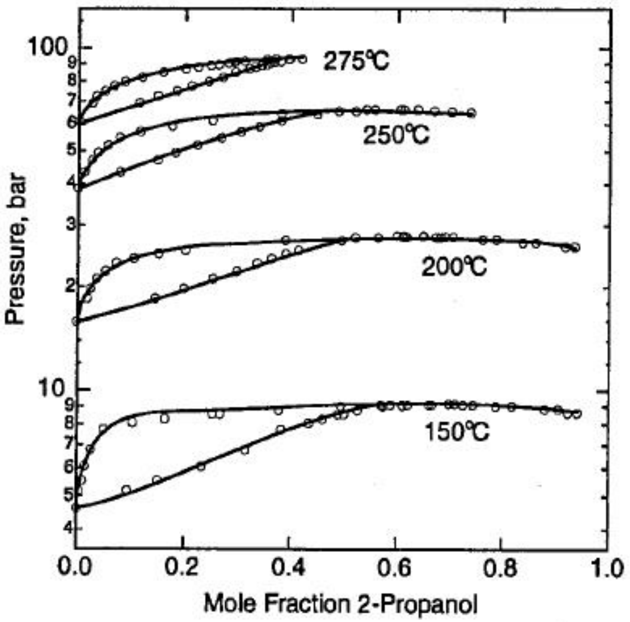

Figure 12-32 High-pressure vapor-liquid equilibria for the binary 2-propanol/water. Calculations from the Peng-Robinson equation, as modified by Stryjek and Vera (1986) using the Wong-Sandler mixing rules (1992) with $k_{12} = 0.326$. —— Calculated; ○ Experiment (Barr-David and Dodge, 1959).

Figure 12-32 compares measured and calculated vapor-liquid equilibria for the binary 2-propanol/water. The calculations were performed with the Peng-Robinson equation of state – with pure component parameters obtained from the correlation of Stryjek and Vera(1986) – using the mixing rules of Wong-Sandler with a_∞^E determined from the can Laar equation.

12.8 Phase Equilibria from a Corresponding-States Correlation

Corresponding-states correlations can be used to calculate fugacities of components in mixtures of normal (nonpolar or slightly polar) fluid.

The general procedure is first, to write a reduced equation of state for compressibility factor z:

$$z = \frac{Pv}{RT} = F_z\left(\frac{T}{T_c}, \frac{P}{P_c}, X\right) \qquad (12\text{-}68)$$

or a reduced equation of state of the form

$$\frac{P}{P_c} = F_P\left(\frac{T}{T_c}, \frac{v}{v_c}, X\right) \qquad (12\text{-}69)$$

Where Tc, Pc, and Vc are critical temperature, pressure, and volume and where X is some additional characteristic parameter such as the acentric factor. Function Fz or Fp may be analytic, tabular or graphical; for computer applications, analytical functions are most convenient.

From Eq. (12-72) or (12-73), we calculate fugacity coefficients as discussed in Chap. 3 [Eqs.(3-14) and (3-53)].

To extend Eqs. (12-68) or (12-69) to mixtures, we use the pseudocritical hypothesis. We find the fugacity coefficient for a component i in the mixture by differentiation; for a binary mixture, fugacity coefficient is found from

$$\ln \varphi_1 = \ln \varphi_{\text{mixt}} + (1 - \mathfrak{z}_1)\left(\frac{\partial \ln \varphi_{\text{mixt}}}{\partial \mathfrak{z}_1}\right)_{T,P} \qquad (12\text{-}70)$$

Where £ is the mole fraction in either the liquid phase or the vapor phase. The condition of vapor-liquid equilibrium is given by Eqs. (12-44) and (12-45).

With one of the most successful corresponding states correlations, Mollerup uses these mixing rules for the critical temperature, critical volume, and acentric factor:

$$T_{c_{\text{mixt}}} = \frac{\sum_i \sum_j z_i z_j v_{c_{ij}} T_{c_{ij}}}{v_{c_{\text{mixt}}}} \tag{12-71}$$

$$v_{c_{\text{mixt}}} = \sum_i \sum_j z_i z_j v_{c_{ij}} \tag{12-72}$$

$$\omega_{\text{mixt}} = \sum_i z_i \omega_i \tag{12-73}$$

with

$$v_{c_{ij}}^{1/3} = \frac{1}{2}\left(v_{c_i}^{1/3} + v_{c_j}^{1/3}\right) \tag{12-74}$$

$$T_{c_{ij}} = (T_{c_i} T_{c_j})^{1/2}(1 - k_{ij}) \tag{12-75}$$

Where kij is a binary parameter characteristic of the i-j interaction. Because calculated results are sensitive to kij, Mollerup has taken much care to find the best values from reliable binary experimental data.

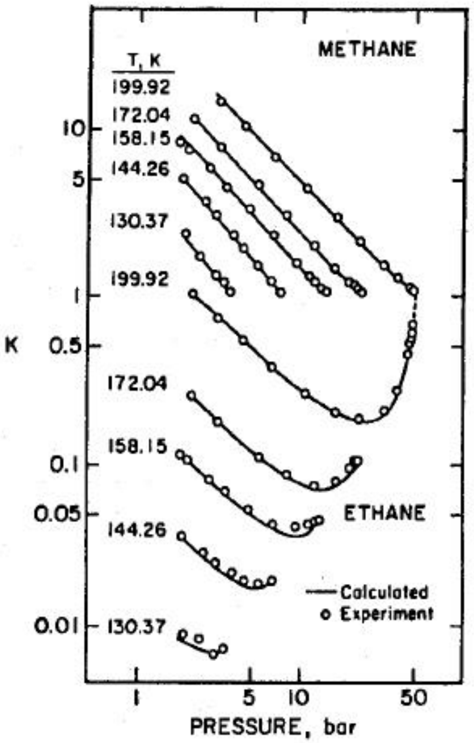

Figure 12-33 *K* factors for the methane/propane system calculated by Mollerup using corresponding-states theory.

Figure 12-33 shows K factors for the methane/propane system calculated by Mollerup.

Another example of how corresponding states may be used to calculate high pressure vapor-liquid equilibria is provided by Plocker′s

$$T_{c_{\mathrm{mixt}}} = \frac{\sum_i \sum_j z_i z_j v_{c_{ij}}^{1/4} T_{c_{ij}}}{v_{c_{\mathrm{mixt}}}^{1/4}} \qquad (12\text{-}76)$$

extension to mixtures of the correlation for pure fluids presented by Lee and Kesler(1975). Plocker found good agreement with experiment upon modifying Eq. (12-75) to read

The exponent 1/4 provides an empirical attempt to take into account that when a small molecule interacts with a large molecule, the small molecule ″sees″ only part of the large molecule.

Plocker also rewrites Eq. (12-75) in the equivalent form

$$T_{c_{ij}} = (T_{c_i} T_{c_j})^{1/2} K_{ij} \qquad (12\text{-}77)$$

where $K_{ij} = 1 - k_{ij}$.

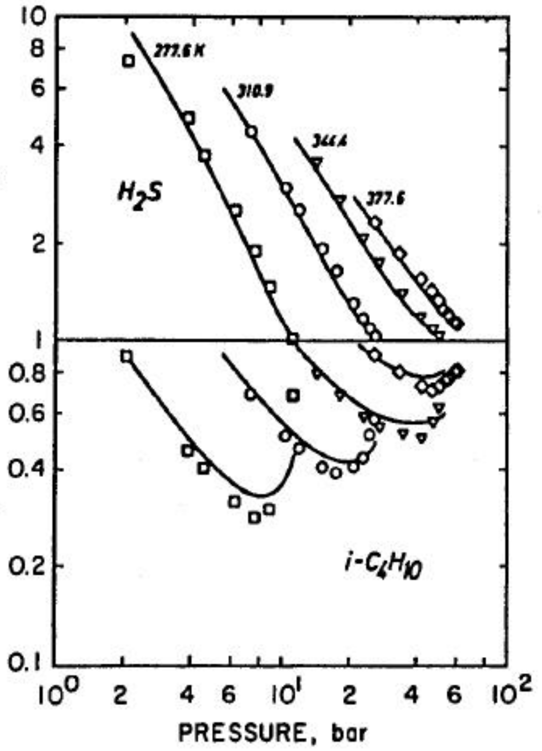

Figure 12-34 Calculated (Plöcker *et al.*, 1978) and experimental (Robinson and Besserer, 1972) *K* factors for the binary system hydrogen sulfide/isobutane.

Figure 12-34 illustrates calculations from Plocker and coworkers using the correlation of Lee and Kesler.

12.9 Vapor-Liquid Equilibria from the Perturbed-Hard-Chain Theory

The perturbed-hard chain(PHC) theory, discussed in Sec. 7.16, can be used to calculate vapor-liquid equilibria at high pressures.

Kim et al. (1982) use the carnahanStarling expression for hard-sphere molecular repulsion [Eq. (7-238)] but for the attractive part they use an expression based on the local-composition model of Lee et al.(1985)
The attractive contribution is

$$z_{\mathrm{att}} = \frac{-Z_{\mathrm{M}}\, v^{*}\left[\exp\left(\frac{1}{2\tilde{T}}\right)-1\right]}{v+v^{*}\left[\exp\left(\frac{1}{2\tilde{T}}\right)-1\right]} \qquad (12\text{-}78)$$

Where Zm is the maximum lattice-site coordination number. For mixtures, Kim used also mixing rules based on van der Waals one-fluid theory.

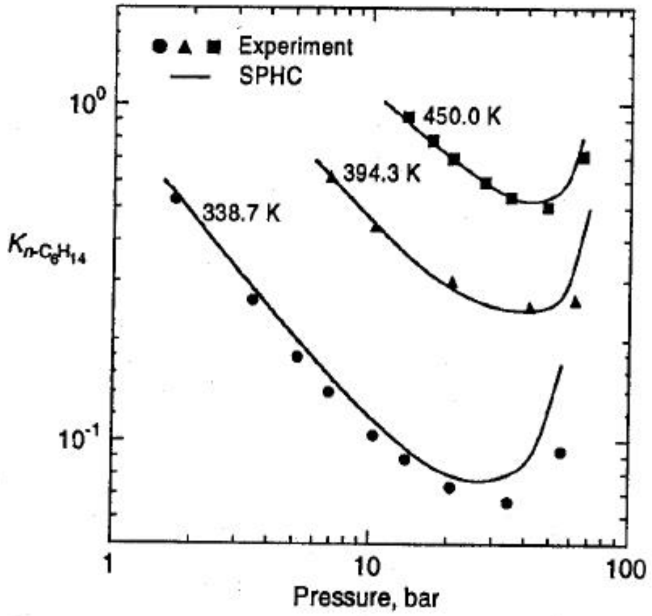

Figure 12-35 Calculated (simplified PHC theory of Kim) and experimental *K* factors for *n*-hexane in the ethane/*n*-hexane binary at 450.0, 394.3, and 338.7 K (Kim *et al.*, 1986).

Figure 12-35 compares calculated with experimental K factors for the ethane/n-hexane system at three temperatures. This K factors were calculated using only pure-component parameters; in this fortuitous case, no adjustable binary interaction parameters are reuired.

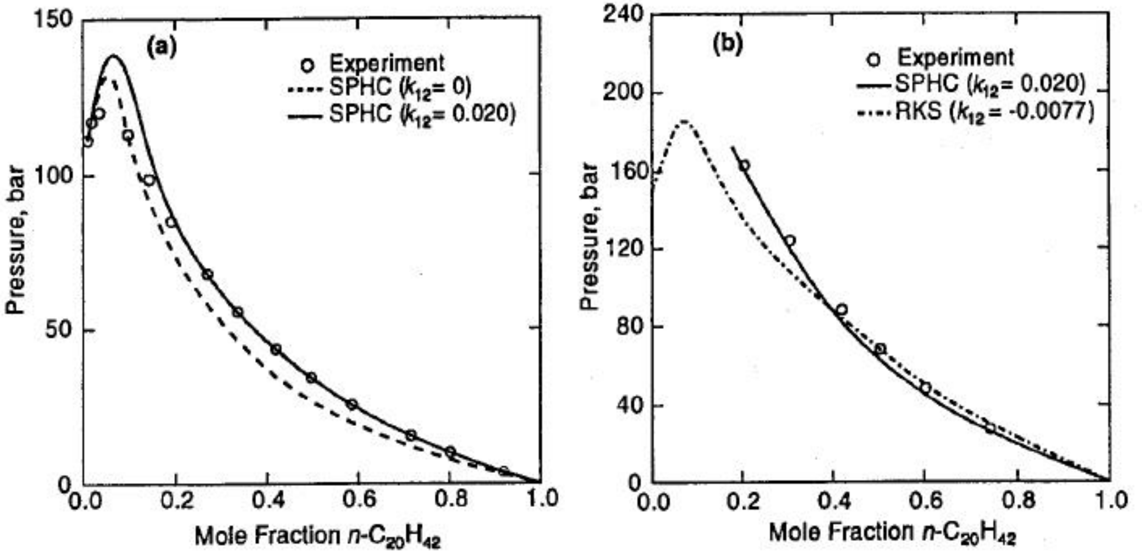

Figure 12-36 Vapor-liquid equilibria for ethane/eicosane at 350.0 K and 450.0 K (Peters *et al.*, 1988). (a) At 350.0 K: o Experiment; - - - - Simplified PHC, $k_{12} = 0$; —— Simplified PHC, $k_{12} = 0.020$; (b) At 450.0 K: o Experiment; —— Simplified PHC, $k_{12} = 0.020$; – - – - – Redlich-Kwong-Soave, $k_{12} = -0.0077$.

However, as Fig. 12-36 shows, to describe vapor-liquid equilibria for mixtures of ethane with a heavy n-alkane, it is necessary to use a binary parameter k_{12} obtained from data regression of the phase envelopes at 350K. Fig. 12-36 shows also calculated results from the Redlich-Kwong-Soave equation of state for the same binary at 450K, but k_{12} optimized at this temperature.

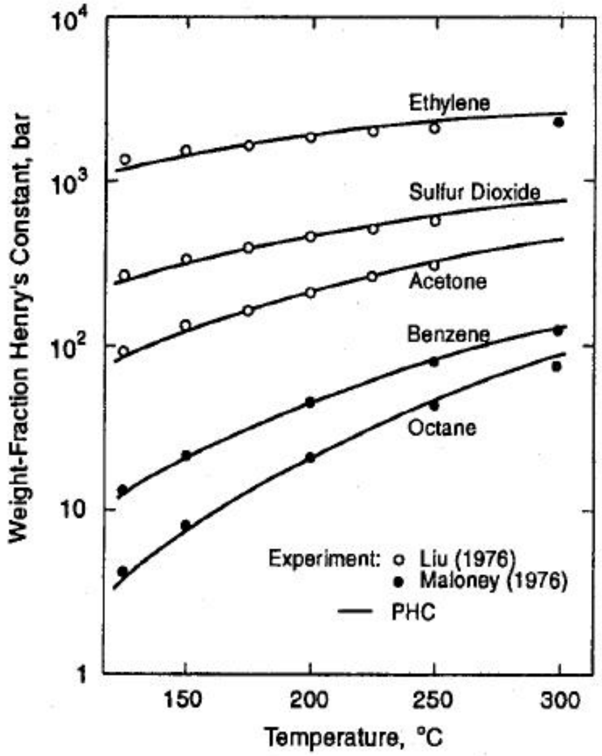

Figure 12-37 Weight-fraction Henry's constants for some solutes in low-density polyethylene. Symbols are experimental data (○ Liu, 1976; ● Maloney, 1976); —— PHC (Cotterman, 1986) with one binary parameter k_{12} per binary system.

Fig. 12-37 shows calculated and observed solubilities (Henry′s constants) for five solutes in low-density polyethylene and Fig. 12-38 shows calculated and observed K factors for a 12-component synthetic oil at 322k with 70mol% carbon dioxide.

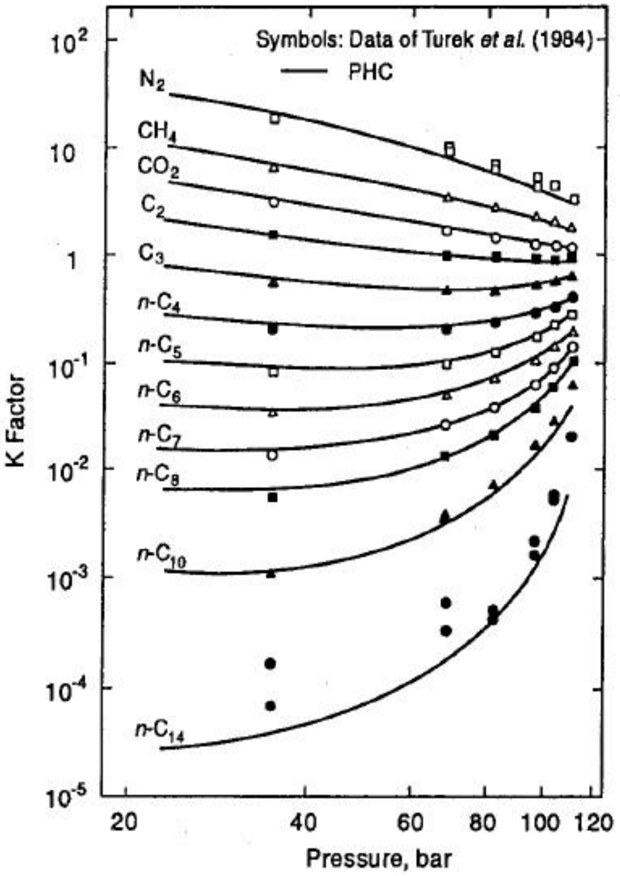

Figure 12-38 *K* factors for 12-component synthetic oil with 70 mol % carbon dioxide at 322 K. Symbols : Experiment (Turek *et al.*, 1984); —— PHC (Cotterman, 1986) with one binary parameter k_{12} per binary system.

12.10 Phase Equilibria Using the Chemical Theory

A classical method to describe strongly non-ideal and associating (hydrogen-bonding) mixtures, is provided by coupling an equation of state with a chemical theory of association and salvation, as indicated in Sec. 5.10. An example of this method is the model of Gmehling based on PHC theory.

The extension takes polar forces into account by assuming that, in addition to the non-ideal properties given by the PHC equation of state, strong polar forces can form dimers. Thus, a binary mixture of A and B is considered to be a five-species mixture containing monomers A and B and, in addition, dimmers A_2, B_2, and AB. The concentrations of these five species are calculated by material balances and by chemical equilibria:

$$K_{A_2} = \frac{\tilde{\gamma}_{A_2}}{\tilde{\gamma}_A^2} \frac{\varphi_{A_2}}{\varphi_A^2 P} \qquad (12\text{-}79)$$

$$K_{B_2} = \frac{\tilde{\gamma}_{B_2}}{\tilde{\gamma}_B^2} \frac{\varphi_{B_2}}{\varphi_B^2 P} \qquad (12\text{-}80)$$

$$K_{AB} = \frac{\tilde{\gamma}_{AB}}{\tilde{\gamma}_A \tilde{\gamma}_B} \frac{\varphi_{AB}}{\varphi_A \varphi_B P} \qquad (12\text{-}81)$$

The equilibrium constants are functions only of temperature. For a binary mixture, fugacity coefficients are calculated from the partition function. Equilibrium constants can be determined from pure-component properties, but K_{AB} must be obtained from binary data. If only A is strongly polar, K_B=K_{AB}=0

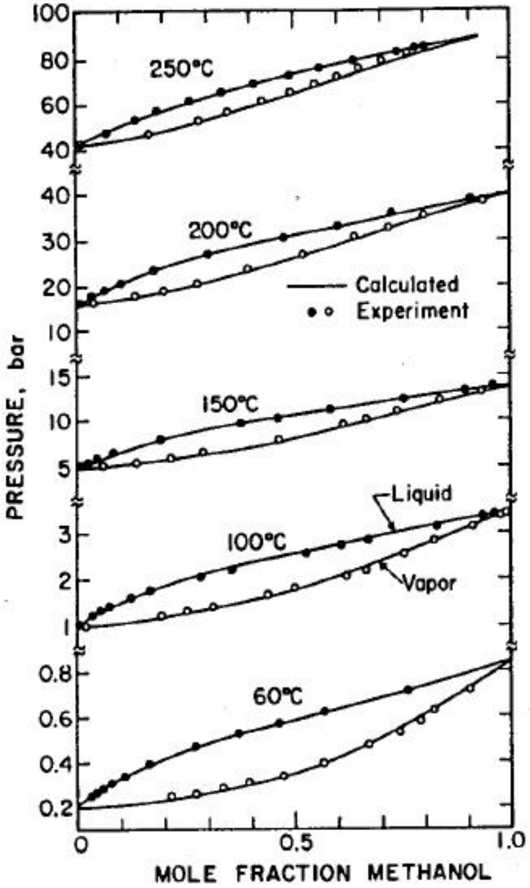

Figure 12-39 Vapor-liquid equilibria for methanol/water (Gmehling *et al.*, 1979).

Figure 12-39 shows calculated and observed equilibria for methanol/water.

The equation of state is separated into its repulsive and attractive contributions,

$$P = P_{\text{rep}} + P_{\text{att}} \tag{12-82}$$

The repulsive term is rewritten in terms of the compressibility factor

$$P_{\text{rep}} = n_T z_{\text{rep}} \frac{RT}{V} \tag{12-83}$$

Where V is the total volume.
The attractive-force contribution in the equation of state is rewritten in the form

$$P_{\text{att}} = -\frac{\hat{a}}{\hat{b}^2} \pi_{\text{att}}(\eta) \tag{12-84}$$

Where π_{att} is a function only of reduced density η. Constant a depends on the composition of the mixture. In the low-density limit, constant a is that of the conventional van der Waals-type equation.

Heidemann postulates a linear association model where a monomer molecule X1 can associate to form dimmers, trimers, etc., according to the chemical equilibria

$$\begin{array}{ccc} X_1 + X_1 & \rightleftharpoons & X_2 \\ X_1 + X_2 & \rightleftharpoons & X_3 \\ \vdots & & \vdots \\ X_1 + X_i & \rightleftharpoons & X_{i+1} \end{array} \tag{12-85}$$

To apply the equation of state to mixtures, the classical mixing rules are

$$\hat{a} = \sum_i \sum_j z_i z_j (a_i a_j)^{1/2} \tag{12-86}$$

$$\hat{b} = \sum_i z_i b_i \tag{12-87}$$

To simplify the model, Heidemann introduce also the following reasonable assumptions

$$a_i = i^2 a \tag{12-88}$$

$$b_i = i b \tag{12-89}$$

Where a and b refer to the monomer.

Conservation of mass relations require that the total number of moles n_T is related to n_0, the number of moles that would exist if there were no association, by

$$n_T \sum_i i z_i = n_0 \tag{12-90}$$

Combination of Eq. (12-90) with Eqs. (12-86) to (12-89) gives

$$\hat{a} = \left(\frac{n_0}{n_T} \right)^2 a \tag{12-91}$$

and

$$\hat{b} = \left(\frac{n_0}{n_T} \right) b \tag{12-92}$$

With the results presented above, we obtain for the equation of state,

$$\boxed{P = \frac{n_T}{n_0} \frac{RT\eta}{b} z_{\text{rep}}(\eta) - \frac{a}{b^2} \pi_{\text{att}}(\eta)} \tag{12-93}$$

To obtain the ratio n_T / n_0 we define the chemical equilibrium constant,

$$K_{i+1} = \frac{\mathfrak{z}_{i+1}}{\mathfrak{z}_i \mathfrak{z}_1} \frac{\varphi_{i+1}}{\varphi_i \varphi_1 P} = \exp\left(-\frac{\Delta h^0}{RT} + \frac{\Delta s^0}{R} \right) \tag{12-94}$$

Obtained from the equation of state {using e.g. Eq. (3-53)}, Δh^0 is the standard enthalpy of association, and ΔS^0 is the standard entropy of association [see Eq. (5-111)].

From material balance equations we find n_T / n_0

$$\frac{n_T}{n_0} = \frac{2}{1 + \sqrt{1 + \frac{4}{v} RTK \exp(g)}} \tag{12-95}$$

We obtain the equation of state for associating fluids

$$\boxed{z = \frac{Pv}{RT} = \frac{2z_{\text{rep}}}{1 + \sqrt{1 + \frac{4}{v} RTK \exp(g)}} - \frac{a\pi_{\text{att}}}{b\eta RT}} \tag{12-96}$$

with

$$g = \int_0^{\eta} \left(\frac{z_{\text{rep}} - 1}{\eta} \right) d\eta \tag{12-97}$$

consider the method proposed by Lencka and Anderko applied to the calculation of vapor-liquid equilibria for the system hydrogen fluoride/$C_2F_3Cl_3$. This system is of technical interest because HF is a byproduct in production of a common refrigerant.

Anderko assumes that the compressibility factor of an associated mixture is separated into a physical and a chemical contribution,

$$z = z_{\mathrm{phys}} + z_{\mathrm{chem}} - 1 \qquad (12\text{-}98)$$

In the mixture, HF can form linear multimers formed by consecutive self-association reactions,

$$(\mathrm{HF})_j + \mathrm{HF} \rightleftharpoons (\mathrm{HF})_{j+1} \quad \text{with} \quad j = 1,2,\ldots,\infty$$

Anderko does not assume that the chemical equilibrium constant is independent of j.
Instead, he uses a distribution function f(j):

$$K_{j,j+1} = f(j)K \qquad (12\text{-}99)$$

The equilibrium constant Ki for the i-merization reaction

$$i\mathrm{HF} \rightleftharpoons (\mathrm{HF})_i \qquad i = 2, 3, \ldots, \infty$$

is related to the consecutive association constants [Eq. (12-99)] by

$$K_i = \left[\prod_{j=1}^{i-1} f(j)\right] K^{i-1} \qquad (12\text{-}100)$$

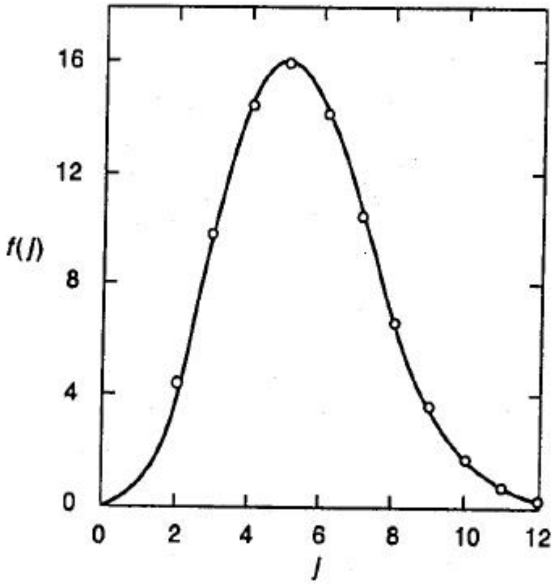

Figure 12-40 Distribution function $f(j)$ proposed by Lencka and Anderko (1993) for hydrogen fluoride. The distribution function shows a maximum near $j = 6$ indicating that HF preferentially forms hexamers.

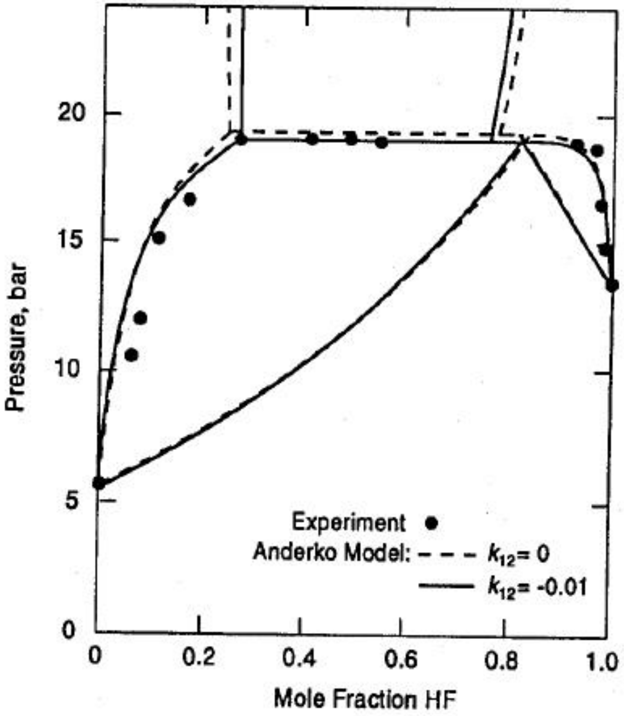

Figure 12-41 Vapor-liquid-liquid equilibria for HF/$C_2F_3Cl_3$ at 383.15 K (Lencka and Anderko, 1993). ● Experiment; —— Association model of Anderko (with k_{12} = -0.01); - - - - Association model of Anderko (with k_{12} = 0).